Forest Recovery after Four Wildfires in Western Montana

A Thesis

Presented in Partial Fulfillment of the requirements for the

Degree of Master of Science

with a

Major in Natural Resources

in the

College of Graduate Studies

University of Idaho

by

Kevin Satterberg

Major Professor: Eva Strand, Ph.D.

Committee Members: Alistair Smith, Ph.D.; Andrew Hudak, Ph.D.

Department Chair: Randy Brooks, Ph.D.

November 2015

Authorization to Submit Thesis

This thesis of Kevin Satterberg, submitted for the degree of Master of Science with a Major in Natural Resources and titled "Forest Recovery after Four Wildfires in Western Montana," has been reviewed in final form. Permission, as indicated by the signatures and dates below, is now granted to submit final copies to the College of Graduate Studies for approval.

Major Professor: _____ Date: _____
Eva Strand, Ph.D.

Committee Members: _____ Date: _____
Alistair Smith, Ph.D.

_____ Date: _____
Andrew Hudak, Ph.D.

Department Administrator: _____ Date: _____
Randy Brooks, Ph.D.

Abstract

Wildfires in mixed conifer forests have increased in size and occurrence over the past decades and are expected to increase in the future because of a warming climate leading to longer fire seasons. To better understand that impacts of wildfires on forests, research focusing on the connection between severity of the fire and forest recovery is needed. Research on immediate fire effects and post-fire recovery within five years of fires have been reported, however long term effects are largely unexplored. To understand long term recovery in mixed conifer forests after wildfire, four wildfires from the 2003 fire season in western Montana were sampled in the field and via remote sensing. Analysis of field data and satellite imagery shows lower tree density in high severity burns and significant differences in recovery rates between severity classes. This research contributes to the scientific knowledge of long term effects of wildfires in mixed conifer forests.

Acknowledgements

This research was supported by the University of Idaho and the United States Forest Service: Rocky Mountain Research Station and the United States Department of Agriculture: Mcintire-Stennis grant. Thank you to those who helped collected field data in both 2013 and 2014. Thank you to the Statistics Assistance Center at the University of Idaho for the guidance on the correct statistical practices. Finally thank you to my colleagues who helped me with my day to day questions about this research.

Table of Contents

Authorizatioin To Submit ii

Abstract iii

Acknowledgements iii

Table of Contents v

List of Figures vii

List of Tables x

CHAPTER 1: IMPACT OF FIRE SEVERITY ON PLANT COMMUNITY RESPONSE AND WILDLAND FUELS IN MIXED CONIFER FORESTS TEN YEARS POST-FIRE 1

- Abstract 1
- Introduction 2
- Methods 6
- Results 15
- Discussion 21
- Conclusions and management implications 27
- References 29

CHAPTER 2: REMOTE SENSING OF FIRE SEVERITY AND POST-FIRE RECOVERY IN MIXED CONIFER FORESTS 36

- Abstract 36

Introduction 36

Methods 41

Results 48

Discussion 62

Conclusion and management implications 66

References 68

Appendix 1 73

Appendix 2 77

Appendix 3 81

Appendix 4 82

List of Figures

Figure 1.1. Locations of wildfires in western Montana and their MTBS severity classifications. The Robert fire footprint contains gaps in the data caused by the failure of the scan line corrector (SLC) onboard Landsat 7 while the other fires were imaged by Landsat 5.. 7

Figure 1.2. Layout of plots at each sampling site. 11

Figure 1.3. Variables that are significant in the MANOVA and significant in the Kruskal-Wallis rank sum test. The bold line represents the sample median, the box represents the first and third quartile of the sample, the whiskers represent the minimum and maximum, and the dots represent outliers..... 17

Figure 1.4. Species and plot locations displayed in ordination space with the severity level for plot locations displayed as a different symbol. Axis 1 shows a positive correlation with mean annual precipitation, fire severity and a negative correlation with annual mean temperature. Therefore, species that are associated with high severity plots are located to the right in the graph and species associated with low severity plots are located at the left side for the graph. 20

Figure 2.1. Map of the locations of the wildfire used in this study including the MTBS severity raster images..... 43

Figure 2.2. NDVI versus years since fire for each of the four BARC severity classes pre- and post-fire. Regression lines (solid) are included for both the pre-fire and the post-fire models. The dashed horizontal line shows the NDVI value of the model the year before the fire. The difference in NDVI recovery time from unburned to high severity was only about 14 years. 50

Figure 2.3. NDVI vs years since fire for each of the four MTBS severity classes pre- and post-fire. Regression lines (solid) are included for both the pre-fire and the post-fire data models. The dashed horizontal line shows the NDVI value the year before the fire, which was the lowest NDVI observed prior to the fire. There was an increase in NDVI recovery time from unburned to high severity of about 3 years..... 51

Figure 2.4. These heatmaps show which severity class recovery models were significantly different from each other for the BARC (left) and MTBS (right) classifications. The white cells are those that are not significantly different from one another and the black cells are significantly different from one another. All classes were significantly different from one another but it is important to note that the MTBS severity is more significantly different than the BARC severity classes are. The numbers in the cells represent the z-scores. 52

Figure 2.5. The above maps show the combination of the severity levels. With BARC being the first severity level and MTBS being the second in each of the classes displayed in the legend. The areas with no change are white and those that had changed are either a red or blue hue. The blue hues represent areas where BARC is a higher severity than MTBS and red represents the opposite. The larger the difference in severity levels the dark the color. The percentage following the combined class name is the percentage of the area that class encompasses. 57

Figure 2.6. Plot of all the NDVI recovery models for randomly selected pixels within combinations of BARC/MTBS classes ranging from unburned to high severity. 58

Figure 2.7. This is a heat map showing what combinations of BARC/MTBS severity were significantly different from one another. The format for the labels is: BARC severity – MTBS severity. The black cells are significantly different from one another (alpha = 0.05) where the grey cells are not. The number in the cell represents the Z-scores..... 59

Figure 2.8. This figure shows the change we observed in aerial photos due to a wildfire. The green circles within the squares are representations of trees within a Landsat pixel. The table shows the percentage of each class combination that followed that path due to a wildfire. 62

List of Tables

Table 1.1. Table showing the number of hectares burned at different severity levels within the fire perimeter of each fire based on remotely sensed data from MTBS. Percentages are reported in parentheses. 8

Table 1.2. Information about the fires included in this research. The fire size is calculated from the final MTBS fire perimeter. The climatic variables are taken from the USFS:RMRS Spline Model of Climate for the Western United States (Rehfeldt 2006) for each of the fires. 8

Table 1.3. Variable group and the F and p values from the non-parametric MANOVA test. For each group there were 999 permutations run, two degrees of freedom, and 31 error degrees of freedom. 15

Table 1.4. All the variables tested using the Kruskal-Wallis rank sum test. All of these tests had two degrees of freedom. The table shows that rock cover, duff depth, percent tree mortality, 1000 hr fuels, and shrub cover were all significant variables at the 0.05 significance level. 16

Table 1.5. The correlation of the explanatory variables to the ordination axis derived from species data. Explanatory variables are: Tree canopy cover (CC), remotely sensed burn severity (dNBR), transformed aspect (TRASP), elevation (DEM), mean annual temperature (MAT), mean annual precipitation (MAP), Julian date of the last freezing date of spring (SDAY), degree-days <0 degrees C (MMINDD0), and summer precipitation balance: (jul+aug+sep)/(apr+may+jun) (SMRPB). Pearson's correlation coefficient, r-squared, and Kendall's tau statistics are reported. 19

Table 2.1. Description of the fires included in this research. The fire size is an estimate from the final MTBS fire perimeter. The climatic variables are taken from the USFS:RMRS Spline Model of Climate for the Western United States (Rehfeldt 2006) for each of the fires. 41

Table 2.2. Landsat image dates for all four wildfires. 45

Table 2.3. Images dates that MTBS used for severity classification. 46

Table 2.4. Images dates that BAER used in creation of BARC maps. A combination of Landsat, Spot, and Aster images were used for these classifications. The Wedge Canyon fire was a single image assessment. 47

Chapter 1: Impact of fire severity on plant community response and wildland fuels in mixed conifer forests ten years post-fire

Abstract

Wildfire is an important ecological process in mixed conifer forests. Wildfires shape forest structure and species composition. To better understand how forests are affected by wildfire, it is common practice in the US to use remotely sensed indicators of fire severity, such as the Normalized Burn Ratio (NBR) maps. Although remotely sensed fire severity indices have been correlated with field assessments of severity immediately after fire, few studies have researched the long term effects of fire severity on forest structure and species composition. We chose four fires that burned in western Montana in 2003, each with varying degrees of severity within the fire perimeter. Data collection included tree density by size class, seedling regeneration, fuel loadings, understory cover, and species composition. Using both Multivariate Analysis of Variance (MANOVA) and ordination indicated that the major difference between the remotely sensed severity classes, ten years post-fire, was the number of live trees. No significant differences were detected between severity classes for fuel loadings, sapling density, seedling density, shrub cover, species diversity or richness. The understory species composition in areas that burned in low or moderate severity was dominated by species with the ability to resprout after fire while areas that burned at high severity contained more species with highly dispersed propagules, with 19 of 148 species exclusively found in high severity burns. Under current climate conditions, we conclude that the mixed-severity fire regime, characterized by a pattern of patches burned at variable

severity, contributes to ecological resilience by increasing gamma heterogeneity and biodiversity in these mixed conifer forests.

Introduction

Fire is an important and complex ecological process in the mixed conifer forests of North America (Agee 1993). Recent research provides evidence that mixed-severity fire regimes were historically widespread in these forests (Odion et al. 2014). Mixed-severity fire regimes contain severity levels ranging from low, moderate, to high distributed in patterns of varying scales across the landscape (Halofsky et al. 2011). This pattern of severity patches originates in variable topography, weather during the fire, and vegetation patterns (Birch et al. 2015). It has been proposed that the patch heterogeneity can contribute to the resilience of mixed conifer forests (Collins & Stephens 2010; Haflofsly et al. 2011) by increasing diversity and intermingling of species. However, it has also been demonstrated that frequently reburned patches can contribute to reduced tree density and alter the ecosystem recovery trajectory (Stevens-Rumann 2015). The high severity fire rotation has been estimated at 200-500 years in mixed conifer forests while the lower severity fire has a shorter rotation (Odion et al. 2014), generally meaning that low and moderate severity fire occurs with a higher frequency at any single location compared to high severity fire (Agee 1993). Fire rotation was defined as the time it takes to burn an area equal in size to the area of interest. Traditionally, mixed conifer forests were thought to be adapted to frequent low/moderate severity fires, however, Odion et al. (2014) presents evidence that areas burned at moderate and high severity commonly occurred in these landscapes. It is understood that high severity fires will have a large impact on the ecosystem than lower

severity fires due to the removal of the oldest group of vegetation, the mature trees. The extended time it takes for trees to recover has a major impact on available sunlight and soil nutrients in the ecosystem.

Fire severity has been discussed widely in fire ecology literature over the past decade and describes a number of physical and biological effects (Lentile et al. 2006; Lentile et al. 2007; Keeley 2009; Morgan et al. 2014). By its broadest definition it is the degree of environmental change incurred by the fire (Keeley 2009). Fire severity can be estimated at several strata in the forest and includes fire effects such as plant mortality, fuel consumption, smoke production, soil heating, and soil water repellency (Morgan et al. 2014). All of these measurements of severity can be measured from the ground, for example using the Composite Burn Index (CBI) (Key & Benson 2006).

To estimate severity for the entirety of a wildfire event data such as satellite imagery are commonly utilized. Pre-and post-fire images of the Normalized Difference Vegetation Index (NDVI; Tucker 1979) or the Normalized Burn Ratio (NBR; Key & Benson 2006) are commonly used to map fire severity across large areas. The difference between pre- and post-fire NBR (dNBR) is documented for all wildfires larger than 500 ha in the US via the Monitoring Trends in Burn Severity (MTBS) project, from 1985 to the present day (Eidenshink et al. 2007). The NBR is computed using the formula:

$$\frac{NIR - SWIR}{NIR + SWIR}$$

Using band 4 for the near infrared (NIR) and band 7 for the short wave infrared (SWIR). MTBS uses the Landsat constellation to estimate fire severity by the dNBR index for

all fires on record. According to MTBS procedures, dNBR represents the difference between pre-fire NBR calculated from an image collected immediately before the fire and post-fire NBR calculated from an image collected one year after the fire by the formula:

$$dNBR = NBR_{prefire} - NBR_{postfire}$$

The dNBR has been shown to correlate well with the loss of biomass and vegetation mortality induced immediately by the fire as well as delayed mortality of trees occurring within the first year post-fire (Key & Benson 2006). Several studies have documented the correlation between dNBR and percent tree mortality in forests (Hudak et al. 2007; Lentile et al.2007; Smith et al. 2010).

Only a few studies have documented relationships between fire severity and understory plant cover including forb, graminoid and shrub cover in mixed conifer forests (Turner et al. 1999; Lentile et al. 2007). Generally, species cover and richness are lower in areas that burn at high severity (Turner et al. 1999; Lentile et al. 2007), at least for a few years following the fire. Turner et al. (1999) found a greater number of forbs following crown fires compared to severe surface fires in mixed conifer forests four years after the 1988 fires in Yellowstone National Park. Turner et al. (1999) further documented that four years after fire, shrub cover was lower at increased fire severity. They also found a higher tree seedling density in areas that burned in surface fires compared to high severity crown fires. The same was discovered for red fir seedlings in Oregon's southern Cascade Mountains where the lowest seedling establishment was observed in high severity areas (Chappell & Agee 1996). These results agree with lab experiments that show high temperatures reduce the survival of seeds in the canopy (Knapp & Anderson 1980; Johnson & Gutsell 1993). To

this date, we have not found any studies recording post-fire vegetation recovery in mixed conifer forests of North America over time periods as long as ten years. This study is therefore unique because it documents changes in forest structure, plant community composition, and wildland fuels ten years after mixed-severity fires in mixed conifer forests in Montana and therefore contributes new knowledge to our understanding of fire severity effects in this forest type.

A better understanding of the effects of fire severity in mixed conifer forests also is important because of expected changes in climate. Consequences of a changing climate include earlier springs resulting in earlier fire seasons and thus a longer fire season (Westerling et al. 2006). Climate change is expected to result in a higher frequency of fires and larger fires (Westerling et al. 2006). Given that the wildland fuels will be dryer, especially the coarse woody debris, these fires may also increase in severity. Fire suppression techniques used in the early- and mid-1900s have left many undeveloped areas with a buildup of fuels (Pyne 1996). Fire effects are generally not consistent across the burned area due to spatial variability in fuel loads, topography, variable weather, and suppression priorities (Kolden et al. 2012; Hayes & Robeson 2013; Strand et al. 2013; Hoff et al. 2014). Considering expected changes in climate and resulting increases in fire occurrence and intensity, Goetz et al. (2007) suggested that further research is required to improve the integration of remotely sensed data, field research, and models to better quantify the long term trajectories of disturbances. To better understand how mixed conifer forests recover after wildfire with variable severity levels, we collected field data ten years post-fire to characterize plant community composition and fuel loads, along a fire severity gradient, in

four fires in western Montana that burned in 2003. Specifically, we collected data to address the following research questions: 1) Does remotely sensed dNBR indicate tree density, establishment of trees, understory plant response, and wildland fuel loads ten years post-fire in mixed conifer forests? 2) Is plant community composition affected by the fire severity level, topographic position, and climate ten years post-fire?

Methods

Study Area

The wildfires incorporated in this study occurred in 2003 in the Northern Rockies of western Montana. The fires can be broken up into two different regions, the northwest fires and the west fires. The northwest fires are the Wedge Canyon and Robert fires that started on July 18th and 23rd respectively. The west fires are the Black Mountain 2 and Cooney Ridge fires that started on August 8th and 9th respectively (Tables 1 and 2). These fires contained all types of fire behavior from crown fire, surface fire, and a mixture of behavior.

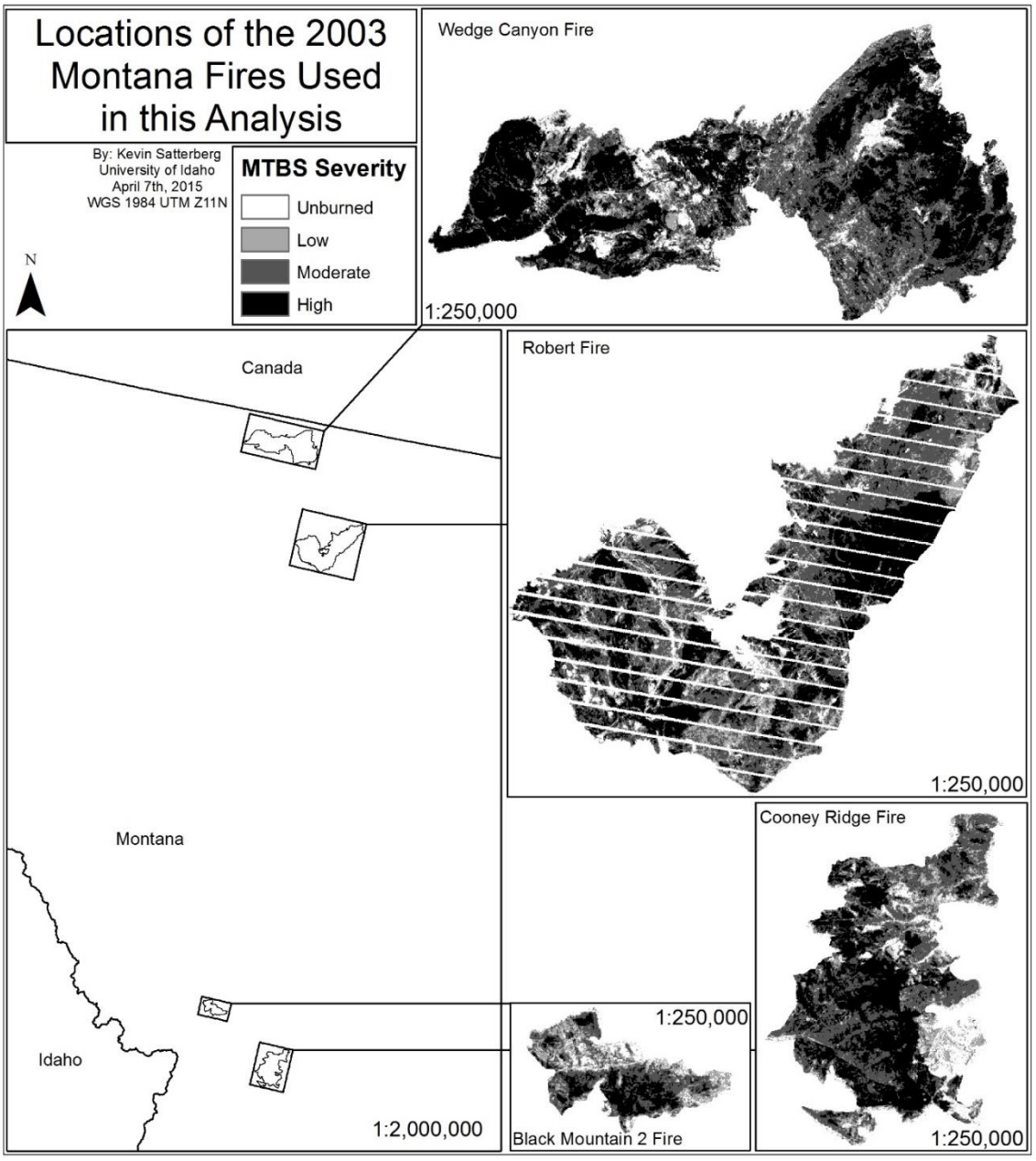

Figure 1. Locations of wildfires in western Montana and their MTBS severity classifications. The Robert fire footprint contains gaps in the data caused by the failure of the scan line corrector (SLC) onboard Landsat 7 while the other fires were imaged by Landsat 5.

Table 1. Table showing the number of hectares burned at different severity levels within the fire perimeter of each fire based on remotely sensed data from MTBS. Percentages are reported in parentheses.

Name	Unburned/low (ha)	Low (ha)	Moderate (ha)	High (ha)	Increased greenness (ha)
Black Mountain 2	634.9 (27.5%)	468.2 (20.3%)	834.8 (36.2%)	364.6 (15.8%)	3.6 (0.2%)
Cooney Ridge	2186.1 (21.4%)	3731.1 (36.5%)	3105.5 (30.4%)	1181.7 (11.6%)	8.5 (0.1%)
Robert	1958.2 (6.0%)	19761.2 (60.9%)	5818.9 (17.9%)	4884.9 (15.0%)	49.8 (0.2%)
Wedge	1335.0 (6.4%)	5361.6 (25.8%)	7517.7 (36.1%)	6587.8 (31.7%)	8.9 (0.0%)

Table 2. Information about the fires included in this research. The fire size is calculated from the final MTBS fire perimeter. The climatic variables are taken from the USFS:RMRS Spline Model of Climate for the Western United States (Rehfeldt 2006) for each of the fires.

Name	Region	Date of Ignition in 2003	Final size (ha)	Elevation (m)	Mean Annual Precipitation (cm)	Mean Annual Temperature (degrees C)
Wedge Canyon	NW	July 18th	21,038	1134-2480	81.5	2.5
Robert	NW	July 23rd	22,055	950-2362	78.5	3.7
Black Mountain 2	W	August 8th	2,996	963-1807	56.1	4.5
Cooney Ridge	W	August 9th	10,417	1125-2318	51.9	3.9

The West region is dryer than the Northwest region by 20 cm of mean annual precipitation from 1971-2000. The driest part of the year for both regions is July and August with the fires in the West receiving the least amount of precipitation (Pfister et al. 1977). The precipitation that occurred in the year before the fire was lower than normal at the western fires and higher at the northwestern fires. Due to the large changes in elevation there is also a large difference in precipitation within each fire, with some higher elevation areas receiving two to three times as much precipitation as some low elevation sites (Pfister et al. 1977).

All four wildfires occurred in mixed conifer forest. The western region is comprised primarily of the Douglas-fir (*Pseudotsuga menziesii)* habitat type (Pfister et al. 1977), dominated by ponderosa pine (*Pinus ponderosa*); however in areas with greater fire suppression there are denser Douglas-fir stands (Cooper et al. 1991). Regionally, the Douglas-fir habitat type in general is thought to have a fire return interval of 15-30 years, however the two western fires have a documented fire return interval of 35-60 years (Arno 1980). The northwestern region fires occurred in a subalpine fir *(Abies lasiocarpa)* habitat type which has a mean fire return interval as low as 90 years for the lower elevations and as high as 150 years in the higher elevation northern aspects (Arno 1980). All four areas hosted lodgepole pine (*Pinus contorta*), western larch (*Larix occidentalis*) and Engelmann spruce (*Picea engelmannii*). Common shrubs included Rocky Mountain maple (*Acer glabrum*), serviceberry (*Amelanchier alnifolia*), myrtle boxwood (*Pachystima myrsinites*), rose (*Rosa* spp.), western thimbleberry (*Rubus parviflorus*), willow species (*Salix* spp.), spiraea (*Spiraea betulifolia*), and huckleberry (*Vaccinium globulare*). Common forbs included common yarrow

(*Achillea millefolium*), pearly everlasting (*Anaphalis margaritacea*), heartleaf arnica (*Arnica cordifolia*), fireweed (*Epilobium angustifolium*), white-flowered hawkweed (*Hieracium albiflorum*), western meadowrue (*Thalictrum occidentale*), round-leaved violet (*Viola orbiculata*), and beargrass (*Xerophyllum tenax*); and common grasses or grass-like species were elk sedge (*Carex geyeri*), pinegrass (*Calamagrostis rubescens*), and blue wildrye (*Elymus glaucus*). Moss and lichen were observed in almost all plots, but were not identified to the species level. A list of all species observed during field data collection can be found in Appendix 1.

Field Data Collection

Field data were collected at all four of these fires. Field data collection sites were stratified by remotely sensed wildfire severity (low, moderate, and high), elevation, and aspect. The elevation and aspect were both classified into two classes using a density slice creating: two classes elevation, low and high; and two classes of aspect, warm and cold, where the warm aspects encompassed azimuths from 120 to 300 degrees and cold aspects encompasses all other aspects.

All field sites were located at least 60 m from the Montana state road layer available from the Montana geographic information clearinghouse (http://geoinfo.msl.mt.gov/). Each field site consisted of five plots (Figure 2), where the central plot was labeled A. The next plot, labeled B, was located upslope from A. The next plot moving clockwise 90 degrees was plot D; moving clockwise another 90 degrees the next plot (downslope from plot A) was labeled F; followed after moving another 90 degrees by plot H (Figure 2). All outer plots B,

D, F, and H were located 30 m from subplot A. At each of the five locations understory vegetation cover by species and fine woody fuels were sampled within a 1x1m quadrat. Ground cover was estimated ocularly by percentage of the quadrat covered by for each class: green vegetation, non-photosynthetic vegetation (NPV, charred and uncharred), rock, and soil. Woody fuels by size class (1 hour (< 2.54 cm in diameter), 10 hour (2.54 – 7.62 cm in diameter), and 100 hour (7.62-20.32 cm in diameter)) were estimated using the photo load technique (Keana & Dickinson 2007). Litter and duff depth were measured in cm at each plot. Forest canopy cover was collected at the plots using a spherical convex densiometer. Data from the densiometer measurements were taken in each cardinal direction at each plot and then averaged.

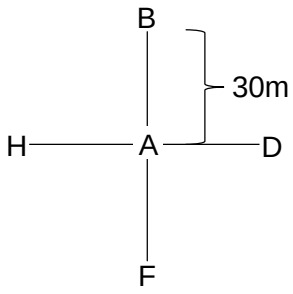

Figure 2. Layout of plots at each sampling site.

Tree data were collected by tallying all the healthy, unhealthy, and dead tree species in an 8-m radius around plot A. Sapling data were collected by counting all the live and dead tree species in a 5.6-m radius around plot A. Saplings are defined as young trees with a stem diameter less than 10 cm at breast height (1.37 m). Seedlings (defined as trees below 1.37 m height but taller than 15 cm) were counted along a belt transect of variable width from F to B; the width as well as the distance along the transect were recorded so seedling counts

could be converted to seedling density (seedlings per hectare). The width of the belt transect and number of 30m segments (ranging from 1-4) was adjusted so the seedling count would be > 30 for the major tree species. Shrub cover taller than breast height was estimated ocularly within the 5.6-m radius sapling subplot centered at plot A. Finally, the 1000 hour (> 20.32 cm in diameter), 100 hour (2.54-7.62 cm), 10 hour (0.64-2.54 cm), and 1 hour (< 0.64 cm) woody fuels were estimated using a photo load guide containing images that show a range of fuel loads (Keana & Dickinson 2007). We then compared what large woody fuels we could see within a 5.6-m radius around plot A to the images and selected the image that looked the most similar to the fuel loads observed on the ground. Field data was collected at a total of 34 locations across the four fires, stratified by the elevation, aspect, and fire severity. There were 9 low severity points, 13 moderate severity points, and 12 high severity points. All data used in the analysis are listed in Appendix 2.

Data analysis

Species richness, the total number of species present including trees, shrubs, grasses, forbs, moss, and lichen, was calculated for each plot and also at the site level. Species diversity was calculated using the Shannon's diversity index (Shannon 1948). Stem counts of trees (live, unhealthy, dead), saplings, and seedlings were converted to stem density measurements in stems per hectare. To consolidate the stem counts of trees measured we computed percent mortality of trees.

We analyzed these data using Multivariate Analysis of Variance (MANOVA) to test for differences in group means of response variables between the severity classes using a non-

parametric method called Permutational Multivariate Analysis of Variance Using Distance Matrices from the Vegan package in the R statistical software (Oksanen et al. 2015; R Core Team 2013). Non-parametric statistics were used because the data did not fulfill the requirements of normality for parametric statistics. We created three groups of variables for analysis based on the scale of data collection: group 1 included the ground cover and species richness; group 2 included fine woody fuels data as well as litter and duff; group 3 included percent tree mortality data, 1000 hour fuels, and shrub cover; and the final group was the same as group 3 but included seedling density. We included 1000 hour fuels in group three because snags become 1000 hour fuels when they fall. For each group there were 999 permutations run to accurately determine statistical significance.

Following the permutation MANOVA, we used another non-parametric method, the Kruskal-Wallis rank sum test of significance (Kruskal & Wallis 2012), to determine if the mean of each response variable was significantly different ($p < 0.05$) between fire severity levels. We used R statistical software (R Core Team 2013) for all statistical analysis.

To analyze the large species dataset, multivariate ordination analysis was used to explore patterns in the plant community composition. Gradient analysis was used to explore gradients of fire severity, dNBR, elevation, cosine transformed aspect (Stage 1976), impact of region (NW and W), and climate in the data using the PCORD software (McCune & Grace 2002). Specifically we used Nonmetric Multidimensional Scaling (NMS), a non-parametric ordination method designed to reveal gradients in species data and correlations with environmental variables. This method was developed after Principal Components Analysis (PCA) was used to analyze species data and is recommended by McCune & Grace (2002) as

the most generally effective ordination method for ecological community data. This method was chosen because it works well with non-normal data, does not assume a linear relationship, and avoids the zero truncation problem that many times occurs with community data (McCune & Grace 2002). NMS is an iterative technique that searches for the solution until it has found a solution within the number of axes given by the user. We used an iterative method described by McCune & Grace (2002) to find the number of axes that corresponded to the lowest stress of just the species data. The axes were then correlated with the primary and secondary matrix using Kendall's tau coefficient (Kendall 1938). The Kendall tau is a non-parametric statistical method to quantify correlation, it is appropriate for data lacking normality. Kendall's tau ranges from -1 to 1, where 0 indicates lack of correlation, a positive number indicates a positive correlation and a negative number indicates a negative correlation. The primary matrix consisted of the cover of species that occurred in a minimum of two stands, 82 species total, and the secondary matrix consisted of the explanatory variables including severity classes, dNBR, elevation, the cosine transformed aspect (Stage 1976), overstory canopy cover, region, and climate variables from the USFS:RMRS Spline Model of Climate for the Western United States (Rehfeldt 2006). These climate variables included: mean annual temperature (MAT), mean annual precipitation (MAP), Julian date of the last freezing date of spring (SDAY), degree-days <0 degrees C (MMINDD0), and summer precipitation balance: (jul+aug+sep)/(apr+may+jun) (SMRPB).

Results

Forest structure and fuels by severity class

Multivariate analysis shows that there are differences in vegetation data between areas that burned at low, moderate, and high severity ten years post-fire. Non-parametric multivariate analysis of variance did not reveal significant differences between low-high severity levels for the understory ground cover data (see group 1 in Table 3). Significant differences were observed in the fuels (see group 2 in Table 3), tree data (see group 3 in Table 3), and tree data plus seedling density (see group 4 in Table 3). When seedling density was included in the tree data (group 4) the difference between severity classes was still significant at alpha = 0.05.

Table 3. Variable group and the F and p values from the non-parametric MANOVA test. For each group there were 999 permutations run, two degrees of freedom, and 31 error degrees of freedom.

Group Number	Variables Used	F	P
1	green vegetation cover, non-photosynthetic vegetation (NPV), charred NPV, rock , soil, and species richness	0.6514	0.530
2	1 hr fuels, 10 hr fuels, 100 hr fuels, litter, and duff	2.9258	0.037
3	% mortality, 1000 hr fuels, and shrub cover	7.1462	0.002
4	% mortality, 1000 hr fuels, shrub cover, and live seedling density	3.4934	0.027

To further evaluate the MANOVA results, we tested the significance of each variable individually with the non-parametric Kruskal-Wallis rank sum test of significance (Table 4). Five variables were significantly different between severity classes those being rock cover,

duff depth, percent tree mortality, 1000 hr fuels, and shrub cover. Figure 3 shows summary statistics for each variable that was significant in the MANOVA and the Kruskal-Wallis rank sum test, and the statistics for all variables collected in the field are summarized in Appendix 3.

Table 4. All the variables tested using the Kruskal-Wallis rank sum test. All of these tests had two degrees of freedom. The table shows that rock cover, duff depth, percent tree mortality, 1000 hr fuels, and shrub cover were all significant variables at the 0.05 significance level.

Variable	Kruskal-Wallis Chi-squared	P value
green cover	1.0773	0.5835
NPV	0.4212	0.8101
NPV charred	2.9127	0.2331
rock	8.4003	0.0150
soil	3.8671	0.1446
species richness	0.5251	0.7691
1 hr fuels	2.5726	0.2763
10 hr fuels	3.6634	0.1601
100 hr fuels	2.6883	0.2608
litter	3.1615	0.2058
duff	8.6696	0.0131
% tree mortality	21.965	0.00002
fuels 1000 hr	13.7547	0.0010
shrub cover	8.6565	0.0131
seedling density	3.4469	0.1785

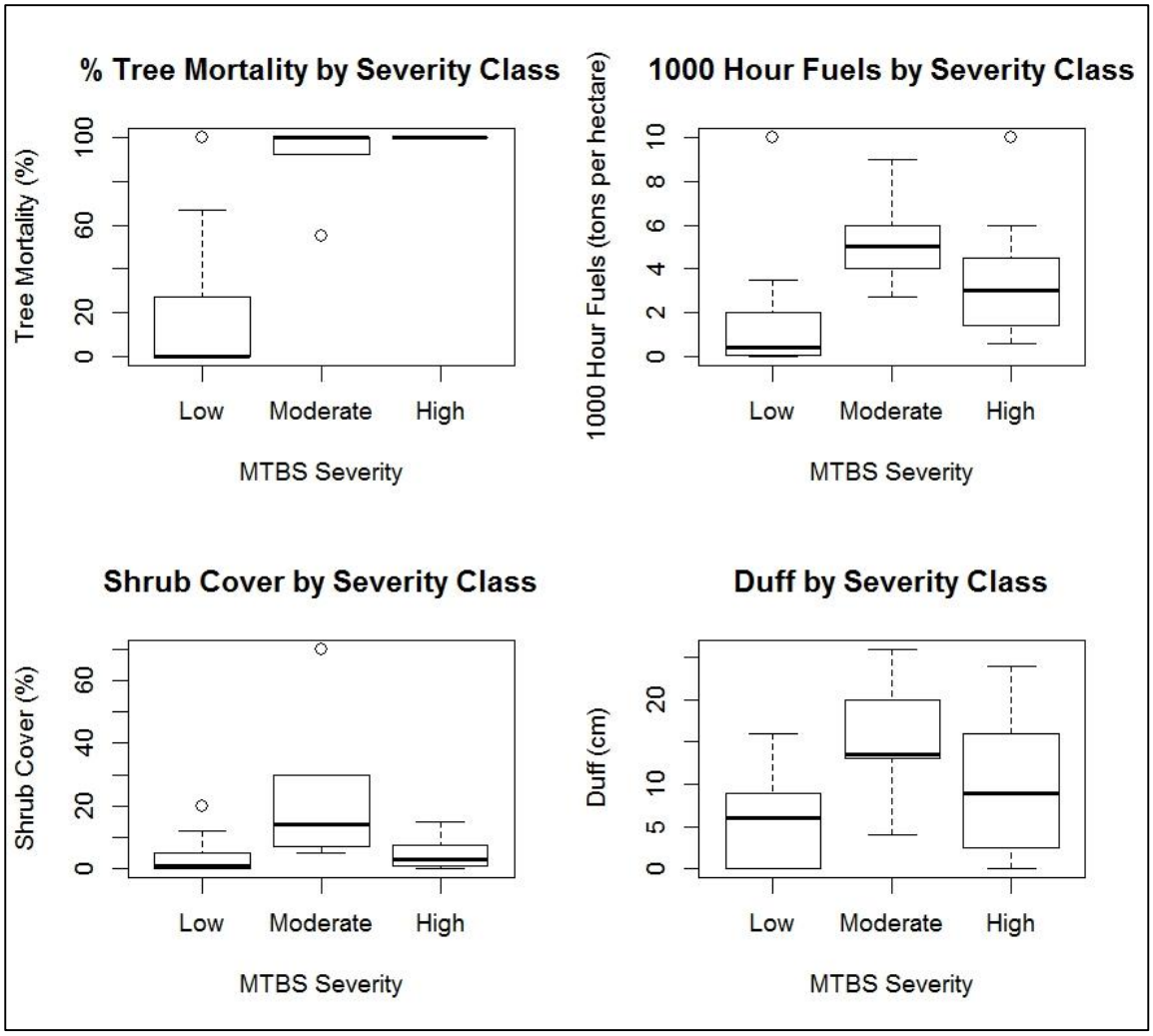

Figure 3. Variables that are significant in the MANOVA and significant in the Kruskal-Wallis rank sum test. The bold line represents the sample median, the box represents the first and third quartile of the sample, the whiskers represent the minimum and maximum, and the dots represent outliers.

Ordination of species data

The NMS ordination method organizes the species data along multiple axes such that species that are similar in ordination space are placed closer together (Figure 4). The first

axis explained 51.4% of the data while the second axis explained 8.1%. A third axis was identified via ordination, however it only explained 3.6% of the data and was therefore excluded from further consideration. To understand correlations between the identified axes, species data, and explanatory variables we looked at the Kendall tau rank correlation coefficient (Kendall 1938) for the explanatory variables (Table 5) and for the individual species (Appendix 4). Correlation with the explanatory variables (Table 5) showed that mean annual precipitation (MAP) was the most important variable explaining axis 1, followed by mean annual temperature (MAT) and remotely sensed burn severity (dNBR). The correlation with MAP was positive while the correlation with MAT was negative, meaning that a high value on axis 1 corresponds to high precipitation and burn severity (dNBR); and low temperatures.

Table 5. The correlation of the explanatory variables to the ordination axis derived from species data. Explanatory variables are: Tree canopy cover (CC), remotely sensed burn severity (dNBR), transformed aspect (TRASP), elevation (DEM), mean annual temperature (MAT), mean annual precipitation (MAP), Julian date of the last freezing date of spring (SDAY), degree-days <0 degrees C (MMINDD0), and summer precipitation balance: (jul+aug+sep)/(apr+may+jun) (SMRPB). Pearson's correlation coefficient, r-squared, and Kendall's tau statistics are reported.

Axis:	1			2			3		
	r	r-sq	tau	r	r-sq	tau	r	r-sq	tau
CC	0.022	0.000	-0.030	-0.269	0.072	-0.167	-0.366	0.134	-0.163
dNBR	0.388	0.151	0.250	0.085	0.007	0.038	0.426	0.182	0.322
TRASP	0.201	0.041	0.189	-0.134	0.018	-0.068	0.039	0.002	0.004
DEM	0.061	0.004	0.106	-0.126	0.016	-0.068	0.473	0.224	0.352
MAT	-0.386	0.149	-0.312	0.075	0.006	0.069	-0.382	0.146	-0.308
MAP	0.539	0.291	0.328	-0.133	0.018	-0.074	0.109	0.012	0.055
SDAY	-0.035	0.001	-0.077	0.079	0.006	0.077	0.312	0.097	0.271
MMINDD0	0.142	0.020	0.102	-0.067	0.005	-0.042	0.405	0.164	0.334
SMRPB	0.035	0.001	-0.058	0.185	0.034	0.116	-0.441	0.194	-0.349

The ordination graph (Figure 4) showed that areas burned at high and low severity respectively had different species compositions but many species occurred in both areas burned at high and low severity. Overall, 148 species were recorded at the 34 field sites, with 119 species recorded on low severity sites, 71 species recorded on moderate severity sites, and 89 species recorded on high severity sites. Of those species 35 were observed *only* in low severity burns, 10 *only* in moderate severity burns, and 19 species were observed *only* in high severity burns. When the cumulative number of species is graphed against the number of plots sampled, the total species richness asymptotes at 148 for the last four plots

and we therefore conclude that the sample size is sufficient to adequately characterize the region with regards to species composition.

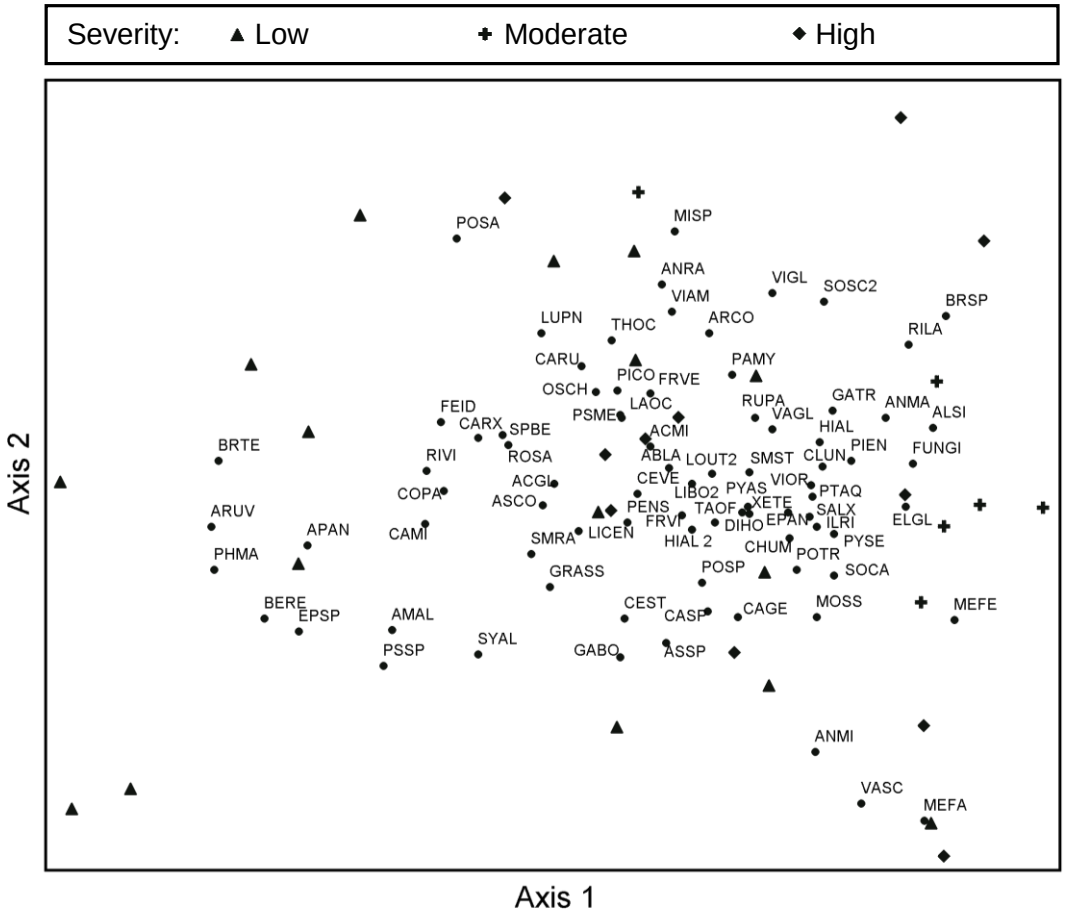

Figure 4. Species and plot locations displayed in ordination space with the severity level for plot locations displayed as a different symbol. Axis 1 shows a positive correlation with mean annual precipitation, fire severity and a negative correlation with annual mean temperature. Therefore, species that are associated with high severity plots are located to the right in the graph and species associated with low severity plots are located at the left side for the graph.

Discussion

Changes in ground cover, fuel loads and tree mortality

Results from multivariate statistical analysis showed that there was no significant difference in ground cover, including green vegetation, NPV, soil, rock, char, or species richness depending on fire severity ten years post-fire in the mixed conifer forest fires sampled in Montana. One year post-fire, in these same fires, Lentile et al. (2007) found that species richness differed between low/moderate severity and high severity patches, with lower richness in high severity burns. They found little difference in species richness between the low and moderate fire severity levels. They also found that the high severity locations had a higher portion of exposed mineral soil than the lower severity patches (Lentile et al. 2007). To mimic the experiments run by Lentile et al. (2007), low and moderate severity were grouped together and were tested against high severity, however ten years post-fire we observed no significant difference in the species richness and exposed mineral soil between the severity groups. Lentile et al's (2007) results are different when compared to our research, and we attribute these differences to the increase in time since fire resulting in adequate time for understory vegetation to recover. The Kruskal-Wallis rank sum tests showed that out of the ground cover group only rock cover was significantly different between severity classes. We believe this is due to the increase exposure of rock post-fire and a large difference in rock cover between high and low severity. Our observations indicated that ten years post-fire, the understory vegetation had recovered to the extent that the differences initially observed between severity levels were no longer detectable using metrics such as species cover, richness, or diversity. Turner et al. (1999) stated that

three years after the 1988 Yellowstone fires the percent biotic cover was back to unburned percentages. Our study agreed with their research that showed no significant effect of severity on understory green cover ten years post-fire. Turner et al. (1999) also found that shrub cover decreased with an increase in fire severity, and tree seedling densities were greater following surface fires compared to crown fires four years post-fire. We observed the highest shrub cover in areas burned at moderate severity (Figure 3), which was different than from Turner et al.'s (1999) findings where shrub cover in a 1 m plot was analyzed. This could be due to the increase in time from the fire to sampling, four years in Turner's study compared to ten years in our research project.

The MANOVA showed a significant difference in fine woody fuel loads (1 hour, 10 hour, 100 hour), litter and duff, across the range of burn severity classes ten years post-fire. In the Kruskal-Wallis rank sum test duff was highly significant and due to this and possibly some interaction effects there was significance in the MANOVA for fuels (group 2). A recent study by Stevens-Rumann (2015) in mixed conifer forests in Idaho did not find a significant difference in fine woody debris fuels in areas burned in high and low severity fires during the time period 2000-2007, which is in agreement with our results. Stevens-Rumann (2015) however, found reduced loads of fine woody debris in forests that had burned more than once in the past 18 years. During these ten years since fire, it is possible that fuels have accumulated to similar loads regardless of burn severity level in our study area. For example, Sah et al. (2006) found that fuel accumulation follows an asymptotic relationship with time, and that in 15-20 years the forest total fuel load has reached its max in Florida Keys pine forests.

The MANOVA showed a significant difference between the fire severity classes ten years post-fire for the combination of percent tree mortality, 1000 hour fuels, and shrub cover (Group 3). All variables in this group were significantly different between severity levels ($p < 0.05$) when the variables were tested separately using the Kruskal-Wallis rank sum test. Clearly, the potential for crown fire has been reduced in areas that burned at high severity because the trees have yet to return to pre-fire heights and density. We included the 1000 hour fuels in the group 3 because they were most likely standing trees before the fire that became snags and logs after the fire, and the size of this coarse woody debris is large enough that ten years is not enough time for them to decompose like fine woody fuels. The density graph (Figure 3) for 1000 hr fuels indicates that there are higher fuel loads in areas that burned in high compared to low severity. The high variability in 1000 hr fuel loads in the moderate severity class obscures these results. In comparison, Stevens-Rumann (2015) found significantly higher 1000 hr fuel loads in high severity burns, compared to the combination of low and moderate severity burns, 8-15 years post-fire. These larger fuels are produced during the burn as trees are killed in the fire but the larger and live sections are not consumed by the flames.

When seedlings were included with the tree variables in MANOVA group 4, the combination of variables continued to be significant. Although in the Kruskal-Wallis rank sum test seedlings alone was not significant. We conclude that all areas in the burned area quickly reseeded after the fire because the fire releases nutrients as well as opens the canopy to increase sunlight to the forest floor. Although there was no significant difference in seedling density between the severity classes, we observed higher seedling densities in

high severity burns compared to low (see seedling density graph in Appendix 3). It should be noted that we observed a large range of seedling density in moderate severity patches. In particular, areas dominated by lodgepole pine prior to the fire had a very high seedling density post-fire. The distance from seed trees within our study ranged from 0 m to 500 m in the sampled plots, suggesting that seed source is not a limiting factor for germination and establishment of new trees in most areas in these four Montana fires. Our results support research by Stevens-Rumann (2015), who found that tree seedling density was significantly correlated with distance to seed-source and with elevation in fires in the Northern Rockies, but that these relationships were independent of fire severity levels.

Turner et al. (1999) showed that areas burned at high severity had the lowest density of seedling re-establishment due to the damage that occurred to the canopy which is the seed source. These results agree with lab experiments that show high temperatures reduces the survival of seeds in the canopy (Knapp & Anderson 1980; Johnson & Gutsell 1993). Turner et al. (1999) found that in the 1988 Yellowstone fire the majority of regeneration occurred between the first and second years, after the fire after which the seedling establishment rate slowed down.

Turner et al. (1999) further found that with increased severity there was a decrease in shrub cover. In the southern cascades of Oregon, Chappell & Agee (1996) found that pre-fire lodgepole dominated stands, where the fire burned at high severity, returned to lodgepole pine dominated stands. The same was not true for areas lacking lodgepole pine; these areas instead were dominated by shrubs post-fire (Chappell & Agee 1996). This could be why we observed the one outlier for a moderate severity plot in the seedling density

graphs (Appendix 3), a site where lodgepole dominated pre-fire and then rapidly returned with a high density of lodgepole pine seedlings. This is due the lodgepole pine cones response to high heat that results from typical moderate or high severity fires.

Understory species composition

The results from the ordination show that fire severity is an important factor impacting the species composition ten years post-fire. Even though species diversity, richness, and cover were not significantly different between the severity classes, 35 species occurred in only low severity, 10 species in only moderate, and 19 species in only high severity. We suggest that the patches of variable fire severity creates a mosaic of post-fire environments that are suitable for establishment of different species, thereby increasing the overall richness and diversity from a landscape perspective. These results support the hypothesis proposed by Halofsky et al. (2011), that mixed-severity fires create a landscape where the close proximity of live and dead forest immediately after the fire, and a fine scale mosaic of early- and late successional plant communities, creates a landscape-level patch mosaic that contributes to resilience within plant communities and thereby potentially by wildlife species.

When we review the species attributes of re-establishment strategies, we noted that species with highly dispersed propagules showed high correlation with the ordination axis 1, representing high severity; while species that reproduce vegetatively or via rhizomes occurred at low to moderate severity on ordination axis 1. For example, we found wind dispersed species such as fire weed (*Epilobium angustifolium*), white-flowered hawkweed

(*Hieracium albiflorum*), and pearly everlasting (*Anaphalis margaritacea*), associated with high severity plots while low severity plots showed sprouting species and species spread by rhizomes more frequently. This includes species such as serviceberry (*Amelanchier alnifolia*), ninebark (*Physocarpus malvaceus*), spiraea (*Spiraea betulifolia*), kinnikinnick (*Arctostaphylos uva-ursi*), and creeping Oregon grape (*Berberis repens*).

High severity fires cause damage to the below-ground plant tissue via soil heating, resulting in a lack of rhizomes, seeds in the seedbank, or other reproductive tissue, available to sprout after the fire (Rowe 1983; Ryan 2002; Stephan et al. 2010). Many of the species that re-established in such areas are wind dispersed, or dispersed by birds or other animals. Low severity areas often have little to no damage to the soil resulting in more of the sprouting and rhizome species in the understory. The moderate severity areas show species with many different re-establishment techniques because moderate severity at this spatial resolution is a conglomeration of fire severity levels and thus fire effects. Many species have multiple modes of reproduction and can re-establish either via sprouting or from seed, e.g. many of the shrubs and rhizomatous forbs and grasses. These species have the ability to rapidly sprout after a low or moderate severity fire or establish via seed after a high severity event; quaking aspen (*Populus tremuloides*) is a good example of such a species.

Our observations in Montana mixed conifer forest follow the relationship between fire severity and the mode of post-fire regeneration proposed by Rowe (1983) and further by Ryan (2002). The ordination (Figure 4) show areas of overlap between severity classes and we believe this is because these species express multiple modes of re-establishment (seed

and sprouting), or they have a broader amplitude than those species that were only in one or two severity polygons.

Conclusions and management implications

We conclude that this research does not suggest that the long term successional trajectory is different for areas that burned in high, moderate, and low severity in the fires studied as part of this project. Comparing the severity levels, the only statistically significant results were groups two through four. The most important of these was group three that contained percent tree mortality, 1000 hr fuels, and shrub cover. With the ordination we noticed that understory species composition dominated by plants with highly dispersed seeds were located in areas that burned at high severity. Tree seedling density and species diversity were not statistically different in areas that burned in high severity compared to low or moderate severity 10 years after the fire. The high seedling density across the burned area indicates that the forest will grow back, given time, unless another fire occurs. We therefore suggest that, although high severity fires result in high tree mortality and longer time for mature trees to occupy the sites, the mixed-severity fires contribute to resilience and diversity at the landscape scale in the forests of Montana. Under a warmer and dryer climate scenario, seedling regeneration could however become a concern (Kemp 2015).

The use of remote sensing indices to determine wildfire severity in mixed conifer forests is related to wildfire effects on trees more so than on surface vegetation. Indices such as dNBR are useful estimating percent tree mortality but do not tell us much about the expected recovery of understory species or trees. Based on our results and as observed by many others (e.g. Smith et al. 2007), areas classified as high severity via remote sensing have

a low live tree density, or in our case a high percent mortality. Across the fires we sampled the tree regeneration was high, however, that may not be the case after all fires, especially in areas that have reburned relatively close together in time (Stevens-Rumann 2015). Remote sensing could therefore be an effective tool in forest management to identify areas for seedling surveys a few years post-fire. If no seedlings are present and trees are desired, then the area could be planted with tree seedlings to speed forest development. To better understand factors impacting tree regeneration following fire, we recommend that future research address the relationship between distance to seed source, seedling regeneration, high severity patch size, and climate.

References

Agee, J. K. (1993). *Fire Ecology of Pacific Northwest Forests*. Washington D.C.: Island Press.

Arno, S. F. (1980). Forest fire history in the northern Rockies. *Journal of Forestry*, *78*, 460–465.

Birch, D. S., Morgan, P., Kolden, C.A, Abatzoglou, J. T., Dillon, G. K., Hudak, A. T. & Smith. A. M. S., 2015. Vegetation, topography and daily weather influenced burn severity in central Idaho and western Montana forests. Ecosphere 6(1), p.17. http://dx.doi.org/10.1890/ES14-00213.1

Chappell, C. B., & Agee, J. K. (1996). Fire Severity and Tree Seedling Establishment in Abies Magnifica Forests, Southern Cascades, Oregon. *Ecological Applications*, *6*(2), 12. Retrieved from http://www.jstor.org/stable/2269397

Collins, B., & Stephens, S. (2010). Stand-replacing patches within a “mixed severity” fire regime: quantitative characterization using recent fires in a long-established natural fire area. *Landscape Ecology*, *25*(6), 927–939. http://doi.org/10.1007/s10980-010-9470-5

Cooper, S. V., Neiman, K. E., & Roberts, D. W. (1991). *Forest habitat types of northern Idaho: a second approximation*. Odgen, UT. Retrieved from http://www.fs.fed.us/rm/pubs_int/int_gtr236.pdf

Eidenshink, J., Schwind, B., Brewer, K., Zhu, Z.-L., Quayle, B., & Howard, S. (2007). A project for Monitoring Trends in Burn Severity. *Fire Ecology*, *3*(1), 3–21.

Goetz, S. J., Mack, M. C., Gurney, K. R., Randerson, J. T., & Houghton, R. A. (2007). Ecosystem responses to recent climate change and fire disturbance at northern high latitudes: observations and model results contrasting northern Eurasia and North America.

Environmental Research Letters, *2*(4), 45031. Retrieved from http://stacks.iop.org/1748-9326/2/i=4/a=045031

Halofsky, J. E., Donato, D. C., Hibbs, D. E., Campbell, J. L., Cannon, M. D., Fontaine, J. B., … Spies, T. A. (2011). Mixed-severity fire regimes: lessons and hypotheses from the Klamath-Siskiyou Ecoregion. *Ecosphere*, *2*(4), art40. http://doi.org/10.1890/ES10-00184.1

Hayes, J. J., & Robeson, S. M. (2013). Spatial Variability of Landscape Pattern Change Following a Ponderosa Pine Wildfire in Northeastern New Mexico, USA. Retrieved from http://www.tandfonline.com/doi/abs/10.2747/0272-3646.30.5.410

Hoff, V., Teske, C. C., Riddering, J. P., Queen, L. P., Gdula, E. G., & Bunn, W. A. (2014). Changes in severity distribution after subsequent fires on the North Rim of Grand Canyon National Park, Arizona, USA. *Fire Ecology*, *10*(2), 48–63.

Hudak, A. T., Morgan P., Bobbitt, M. J. Smith, A. M. S., Lewis, S. A., Lentile, L. B., Robichaud, P. R., Clark, J. T. & McKinley, R. A., 2007. The relationship of multispectral satellite imagery to immediate fire effects. Fire Ecology 3(1) p.64–90.

Johnson, E. A., & Gutsell, S. L. (1993). Heat budget and fire behaviour associated with the opening of serotinous cones in two Pinus species. *Journal of Vegetation Science*, *4*(6), 745–750. http://doi.org/10.2307/3235610

Keana, R. E., & Dickinson, L. J. (2007). *Photoload Sampling Technique: Estimating Surface Fuel Loading From Downward Looking Photographs of Synthetic Fuelbeds*.

Keeley, J. E. (2009). Fire intensity, fire severity and burn severity: a brief review and suggested usage. *International Journal of Wildland Fire*. Retrieved from http://dx.doi.org/10.1071/WF07049

Kemp, Kerry, 2015. Wildfire and Climate Change in Mixed-Conifer Ecosystems of the Northern Rockies: Implications for Forest Recovery and Management Dissertation, College of Natural Resources, University of Idaho, Moscow, Idaho.

Kendall, M. G. (1938). A New Measure of Rank Correlation. *Biometrika*, *30*(1/2), 81–93. http://doi.org/10.2307/2332226

Key, C. H., & Benson, N. C. (2006). *Landscape assessment: ground measure of severity, the Composite Burn Index, and remote sensing of severity, the Normalized Burn Ratio. FIREMON: Fire Effects Monitoring and Inventory System. Gen. Tech. Rep. RMRS-GTR-164-CD* (Vol. USDA Fores). Ogden, UT: USDA Forest Service, Rocky Mountain Research Station: LA 1–51.

Knapp, A. K., & Anderson, J. E. (1980). Effect of Heat on Germination of Seeds from Seotunous Lodgepole Pine Cones. *American Midland Naturalist*, *104*(2), 2. Retrieved from http://www.jstor.org/stable/2424879

Kolden, C. A., Lutz, J. A., Key, C. H., Kane, J. T., & van Wagtendonk, J. W. (2012). Mapped versus actual burned area within wildfire perimeters: Characterizing the unburned. *Forest Ecology and Management*, *286*(0), 38–47. http://doi.org/http://dx.doi.org/10.1016/j.foreco.2012.08.020

Kruskal, W. H., & Wallis, W. A. (2012). Use of Ranks in One-Criterion Variance Analysis. Retrieved from http://www.tandfonline.com/doi/abs/10.1080/01621459.1952.10483441

Lentile, L. B., Holden, Z. A., Smith, A. M. S., Falkowski, M. J., Hudak, A. T., Morgan, P., … Benson, N. C. (2006). Remote sensing techniques to assess active fire characteristics and post-fire effects. *International Journal of Wildland Fire*. Retrieved from http://dx.doi.org/10.1071/WF05097

Lentile, L. B., Morgan, P., Hudak, A. T., Bobbitt, M. J., Lewis, S. A., Smith, A. M. S., & Robichaud, P. R. (2007). Post-fire burn severity and vegetation response following eight large wildfires across the Western United States. *Fire Ecology*, *3*(1), 91–108. Retrieved from http://www.treesearch.fs.fed.us/pubs/29509

McCune, B., & Grace, J. B. (2002). *Analysis of Ecological Communities*.

Morgan, P., Keane, R. E., Dillon, G. K., Jain, T. B., Hudak, A. T., Karau, E. C., … Strand, E. K. (2014). Challenges of assessing fire and burn severity using field measures, remote sensing and modelling. *International Journal of Wildland Fire*, *23*(8), 1045. http://doi.org/10.1071/WF13058

Odion, D. C., Hanson, C. T., Arsenault, A., Baker, W. L., DellaSala, D. a., Hutto, R. L., … Williams, M. a. (2014). Examining historical and current mixed-severity fire regimes in ponderosa pine and mixed-conifer forests of western North America. *PLoS ONE*, *9*(2), e87852. http://doi.org/10.1371/journal.pone.0087852

Oksanen, J., Blanchet, F. G., Kindt, R., Legendre, P., Minchin, P. R., O'Hara, R. B., … Wagner, H. (2015). vegan: Community Ecology Package. Retrieved from http://cran.r-project.org/web/packages/vegan/index.html

Pfister, R. D., Kovalchik, B. L., Arno, S. F., & Presby, R. C. (1977). *Forest habitat types of Montana.* Ogden, Utah: US Department of Agriculture, Forest Service, Intermountain Forest and Range Experiment Station. Retrieved from http://www.fs.fed.us/rm/pubs/rmrs_gtr292/1980_arno.pdf

Pyne, S. J. (1996). *Introduction to Wildland Fire* (2nd ed.). Hoboken, NJ: John Wiley & Sons, Incorporated.

R Core Team. (2013). R: A language and environment for statistical computing. Vienna, Austria. Retrieved from http://www.r-project.org/

Rehfeldt, G. L. (2006). *A spline model of climate for the Western United States.* Fort Collins, CO. URL http://forest.moscowfsl.wsu.edu/climate/customData/.

Rowe, J. S. (1983). Concepts of fire effects on plant individuals and species. In *The role of fire in northern circumpolar ecosystems.* (pp. 135–154).

Ryan, K. C. (2002). Dynamic Interactions between Forest Structure and Fire Behavior in Boreal Ecosystems. *Silva Fennica*, *36*(1), 13–39.

Sah, J. P., Ross, M. S., Snyder, J. R., Koptur, S., & Cooley, H. C. (2006). Fuel loads, fire regimes, and post-fire fuel dynamics in Florida Keys pine forests. *International Journal of Wildland Fire*. Retrieved from http://dx.doi.org/10.1071/WF05100

Schoennagel, T., & Nelson, C. R. (2010). Restoration relevance of recent National Fire Plan treatments in forests of the western United States. *Frontiers in Ecology and the Environment*, *9*(5), 271–277. http://doi.org/10.1890/090199

Shannon, C. E. (1948). A mathematical theory of communication. *Bell System Technical Journal, The*. http://doi.org/10.1002/j.1538-7305.1948.tb01338.x

Smith, A. M. S., Lentile, L. B., Hudak, A. T., & Morgan, P. (2007). Evaluation of linear spectral unmixing and ΔNBR for predicting post-fire recovery in a North American ponderosa pine forest. *International Journal of Remote Sensing*, 28(22), 5159–5166. http://doi.org/10.1080/01431160701395161

Smith, A.M. S., Eitel, J.U. H. & Hudak, A.T., 2010. Spectral analysis of charcoal on soils: implications for wildland fire severity mapping methods. *International Journal of Wildland Fire,* 19(7), p. 976-983.

Stage, A. R. (1976). An expression for the effect of aspect, slope, and habitat type on tree growth. *Forest Science*, *22*(4), 4.

Stephan, K., M., M., & Dickinson, M. B. (2010). First-order fire effects on herbs and shrubs: present knowledge and modeling needs. *Fire Ecology*, *6*(1), 95–114.

Stevens-Rumann, C., 2015. Prior wildfires influence burn severity of subsequent wildfires. Dissertation, College of Natural Resources, University of Idaho, Moscow, Idaho.

Strand, E. K., Bunting, S. C., & Keefe, R. F. (2013). Influence of Wildland Fire Along a Successional Gradient in Sagebrush Steppe and Western Juniper Woodlands. *Rangeland Ecology & Management*, *66*(6), 667–679. http://doi.org/10.2111/REM-D-13-00051.1

Tucker, C. J. (1979). Red and photographic infrared linear combinations for monitoring vegetation. *Remote Sensing of Environment*, *8*(2), 127–150. http://doi.org/10.1016/0034-4257(79)90013-0

Turner, M. G., Romme, W. H., & Gardner, R. H. (1999). Prefire Heterogeneity, Fire Severity, and Early Postfire Plant Reestablishment in Subalpine Forests of Yellowstone National Park, Wyoming. *International Journal of Wildland Fire*, *9*(1), 15. Retrieved from http://landscape.zoology.wisc.edu/People/Turner/Turner1999_IJWF.pdf

Westerling, A. L., Hidalgo, H. G., Cayan, D. R., & Swetnam, T. W. (2006). Warming and Earlier Spring Increase Western U.S. Forest Wildfire Activity. *Science*, *313*(5789), 940–943. http://doi.org/10.1126/science.1128834

Chapter 2: Remote Sensing of Fire Severity and Post-Fire Recovery in Mixed Conifer Forests

Abstract

With the increase of area burned in wildfires due to climate change, it is important to understand how these fires affect our forests. Earth orbiting satellites have been used to assess wildfires over the last few decades, specifically the Landsat satellite constellation has been used to assess wildfire effects on vegetation. Current fire severity products are produced from Landsat imagery to assess impacts on forest soils and vegetation. These products are provided by the Burned Area Emergency Response (BAER) and the Monitoring Trends in Burn Severity (MTBS) projects. The BAER products are created to quickly assess the soils and their susceptibility to erosion. The MTBS products are used for one-year post-fire assessment of fire effect on the vegetation. Currently there is a lack of research investigating wildfire effects on vegetation for five or more years after the fire. The goal of this research is to create a methodology that uses freely available data to assess long- term wildfire effects on forests. This research documents the time required to return to pre-fire reflectance values for four wildfires that burned at mixed-severity levels in mixed conifer forests in western Montana. Significant differences in recovery time between MTBS burn severity classes were observed.

Introduction

Forest wildfires impact both biological and social systems. Wildfire alters vegetation composition and structure with consequences for wildlife habitat (Smith & Fischer 1997; Vierling et al. 2008; Seavy & Alexander 2014). Plant community composition is often altered because species adaptation to fire is variable; for example, some species require fire to

sprout or germinate and establish, while other species have a low tolerance to fire (Stephan et al. 2010). The atmosphere is affected by the release of greenhouse gasses during the flaming and smoldering phases of combustion (Pyne 1996), and the timber that was once standing and holding carbon releases a portion of it to the atmosphere and to decay into the lithosphere. Timber resources may be lost due to wildfire and recreational opportunities are often temporarily affected by reduction in vegetation and wildlife after the fire (Stein et al. 2013). With federal wildfire suppression costs approaching the billions it is imperative that we study what impacts fire inflicts on the vegetation (National Interagency Fire Center 2015) both short and long term.

Global climate change is predicted to occur over the next few decades (Solomon et al. 2007). Consequences of a changing climate include earlier springs resulting in earlier fire seasons thus a longer fire season (Westerling et al. 2006). These changes are predicted to result in a higher frequency of fires and larger fires occurring (Westerling et al. 2006), with the greatest changes predicted in the low elevation forests of the Northern Rockies. Fire suppression techniques used in the early and mid 1900s have left many undeveloped areas with a buildup of fuels (Pyne 1996). When a fire occurs the burn is generally not consistent across the burned area due to spatial variability in fuel loads, topography, variable weather, and suppression priorities (Hayes & Robeson 2013; Kolden et al. 2012; Hoff et al. 2014; Strand et al. 2013). Within the fire perimeter there are areas that burn at different severity levels, impacting plant mortality, seedbanks, soil properties and post-fire recovery (Stephan et al. 2010).

Fire severity is measured in a number of different ways (Lentile et al. 2007; Key & Benson 2006; Morgan et al. 2014). Protocols for ground measurements, such as the Composite Burn Index (CBI; Key & Benson 2006) are used by field crews to assess fire severity at different strata ranging from the soil to the upper tree canopy. Another common method is the use of spectral indices derived from data obtained from satellite sensors to estimate fire severity. There are two common indices for measuring fire severity from satellite and those are the Normalized Burn Ratio (NBR) and the Normalized Difference Vegetation Index (NDVI). The most frequently used index is the NBR that takes the Shortwave Infrared (SWIR) band and subtracts it from the Near Infrared (NIR) band to create a multi-spectral index of fire severity (M.J. & Caselles 1991). NBR is computed using the formula:

$$\frac{NIR - SWIR}{NIR + SWIR}$$

The difference between NBR pre-fire and post-fire, the difference normalized burn ratio (dNBR) value, shows the difference between burned and unburned pixels and has been classified into a range of severity levels. The dNBR is computed using the formula:

$$dNBR = NBR_{prefire} - NBR_{postfire}$$

There are two ways that dNBR is calculated: 1) The initial assessments are used by federal agency teams such as the Burned Area Emergency Response (BAER) teams to prioritize areas that are in need of post-fire rehabilitation. These initial assessments are created with one post-fire NBR image obtained immediately after the fire subtracted from a pre-fire image that is often taken the year before the wildfire around the same date as the

post-fire image. For the BAER teams a Burned Area Reflectance Classification (BARC) map is produced as soon as possible after the wildfire following the initial assessment method. This means often times that there is smoke, or clouds in the satellite image causing analysis errors. 2) The extended assessments computes a dNBR that uses a one year anniversary image and subtracts it from a pre-fire image immediately pre-fire (Brewer et al. 2005). The Monitoring Trends in Burn Severity (MTBS) project has published extended assessments on all fires that occurred since 1984 (Eidenshink et al. 2007). The extended assessment is produced under less time constraint compared to the BARC maps and there is often little to no clouds or smoke in the images. For both the immediate and extended assessment it is important to keep the Julian date or day of the year close to one another to reduce variations caused by phenology (Key & Benson 2006).

Fire behavior and effects can vary greatly across vegetation types. Variations in phenology and productivity are more pronounced in dry grasslands where large variations in precipitation are common. When these grasslands burn they burn with a moderate to high rate of spread thus there is little to no residence time to create a large heat pulse into the soil (Scott & Burgan 2005). This means that the below-ground tissue of many perennial grasses and forbs, and sprouting shrubs, survive the fire and only the above-ground portion of the vegetation is removed. In forested systems with minimal fuels buildup and lack of ladder fuels, low intensity surface fires only consume a portion of the biomass on the forest floor. If fire enters the forest canopy there can be much damage done to the trees from crown scorch and from a long lasting smoldering surface fire resulting in a larger heat pulse into the base of the tree that can kill trees by damaging the cambium (Reinhardt et al. 1997).

Several studies have documented the correlation between dNBR and percent tree mortality in forests (Hudak et al. 2007; Lentile et al. 2007; Smith et al. 2010). Further research has been focusing on high severity crown fires resulting in a forested system that takes much longer to return to a pre-fire state after the wildfire (Lannom et al. in review).

Recent research quantifying post-fire forest recovery using remote sensing has been conducted by Lannom et al. (in review) where they created a chronosequence of recovery for extreme fires in the western US using Landsat imagery. They used a technique of swapping space for time to quantify recovery for fires that occurred from the 1910 fire up to the 2007 East Zone complex fire in central Idaho. Lannom et al. (in review) limited the analysis area to high severity locations only. Our study expands on the research conducted by Lannom et al. (in review) by studying differences in recovery rates between severity levels. We analyzed a post-fire recovery chronosequence of Landsat images for four wildfires that occurred in 2003 using severity metrics from two different sources (BARC and MTBS).

This research, conducted in mixed conifer forests with a mixed-severity fire regime in western Montana, was motivated by three research questions:

1) Is the post-fire recovery rate, i.e. the time it takes for the ecosystem to return to pre-fire NDVI, different for different remotely sensed fire severity levels?; 2) How long does it take for burned areas in different fire severity classes to return to pre-fire NDVI?; 3) Is the initial (BARC) or extended (MTBS) fire severity assessment, or a combination of the two, a better indicator of what the recovery rate will be in mixed conifer forests?

Methods

Study area

The wildfires incorporated in this study occurred in 2003 in the Northern Rockies of western Montana. The fires can be broken up into two different groups, the northwest fires and the west fires. The northwest fires are the Wedge Canyon and Robert fires that started on July 18th, and July 23rd respectively. The west fires are the Black Mountain 2 and Cooney Ridge fires that started on August 8th, and August 9th respectively (Table 1, Figure 1). These fires contained all types of fire from crown fire down to surface fire. All of the fires were ignited by lightning.

Table 1. Description of the fires included in this research. The fire size is an estimate from the final MTBS fire perimeter. The climatic variables are taken from the USFS:RMRS Spline Model of Climate for the Western United States (Rehfeldt 2006) for each of the fires.

Name	Region	Date of Ignition in 2003	Final size (ha)	Elevation (m)	Mean Annual Precipitation (cm)	Mean Annual Temperature (degrees C)
Wedge Canyon	NW	July 18th	21,038	1134-2480	81.5	2.5
Robert	NW	July 23rd	22,055	950-2362	78.5	3.7
Black Mountain 2	W	August 8th	2,996	963-1807	56.1	4.5
Cooney Ridge	W	August 9th	10,417	1125-2318	51.9	3.9

The West region is dryer than the Northwest region by about 10 cm of precipitation for the average yearly precipitation from 1971-2000. The driest part of the year for both regions is July and August with the fires in the West receiving the least amount of precipitation (Pfister et al. 1977). The precipitation that occurred in the water year before the fire was lower than the normal at the western fires and higher at the northwestern fires. Due to the large changes in elevation there is also a large difference in precipitation within each fire, some higher elevation areas have two to three times as much precipitation as those low elevation sites (Pfister et al. 1977).

All four wildfires occurred in mixed conifer forest. The burned areas in the forests of the western region are composed of Douglas-fir (*Pseudotsuga menziesii)* habitat type (Pfister et al. 1977), which is dominated by ponderosa pine (*Pinus ponderosa*); however in areas with greater fire suppression there are denser Douglas-fir stands (Cooper et al. 1991). The Douglas-fir habitat type has a fire return interval of 15 to 30 years, however the western region of this study have a fire return interval of 35-60 years according to Arno (1980). The northwestern region fires occurred in a subalpine fir *(Abies lasiocarpa)* habitat type which has a mean fire return interval as low as 90 years for the lower elevations and as high as 150 years in the higher elevation northern aspects (Arno 1980). All four areas hosted lodgepole pine (*Pinus contorta*), western larch (*Larix occidentalis*) and Engelmann spruce (*Picea engelmannii*).

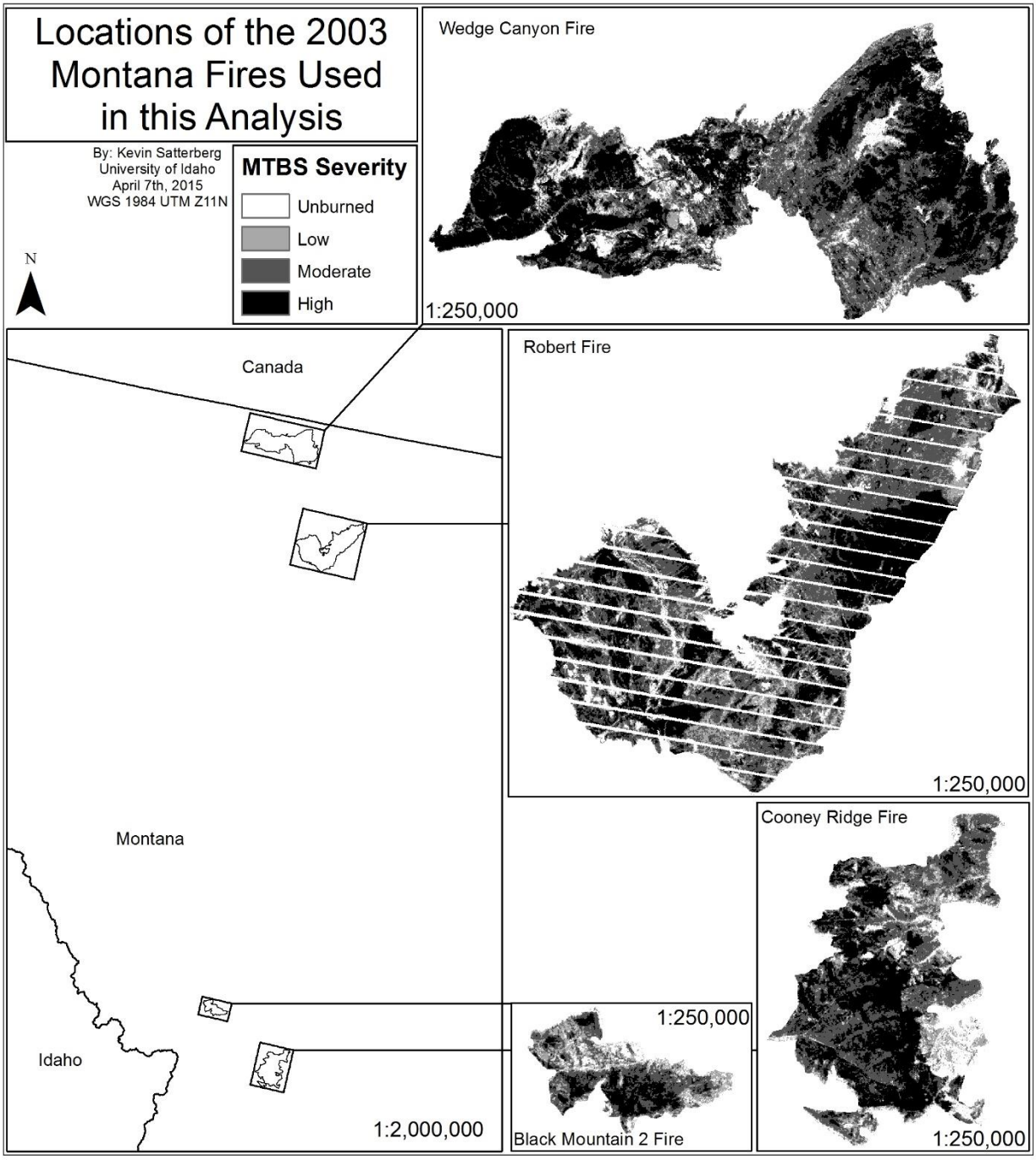

Figure 1. Map of the locations of the wildfire used in this study including the MTBS severity raster images.

Data

Multiple sources of data were used in this research including: Landsat imagery, Monitoring Trends in Burn Severity (MTBS), LANDFIRE, and Burned Area Reflectance Classification (BARC). The Landsat data were obtained from the Landsat Climate Data Record (CDR). All data provided by the CDR were delivered as surface reflectance using the LEDAPS software (Masek et al. 2006). This software geometrically, radiometrically, and atmospherically corrects the data, therefore no preprocessing was necessary, except to scale the values from integers of reflectance into real numbers of reflectance. To remove the interference caused by clouds, water, and ice the mask provided by the CDR was used to exclude these areas from analysis. The Landsat data were transformed into the Normalized Difference Vegetation Index (NDVI) to represent the amount leaf area of each pixel (Tucker 1979) and in turn the amount of photosynthesis occurring (Myneni et al. 1995). NDVI layers were derived from Landsat images of the burned area five years prior to the 2003 fire and 11 years following the fire.

Table 2. Landsat image dates for all four wildfires.

Fire Name	Image Dates
Wedge Canyon and Robert	July 7th, 1998; July 26th, 1999; July 12th, 2000; June 29th, 2001; July 18th, 2002; July 23rd, 2004; July 26th, 2005; July 13th, 2006; August 1st, 2007; July 18th, 2008; July 21st , 2009; July 8th, 2010; August 12th, 2011; August 6th, 2012; July 16th, 2013; August 4th, 2014
Black Mountain 2	July 23rd, 1998; July 26th, 1999; July 12th, 2000; August 16th, 2001; July 18th, 2002; July 23rd, 2004; July 26th, 2005; July 29th, 2006; July 16th, 2007; July 18th, 2008; July 21st, 2009; July 24th, 2010; July 11th, 2011; August 22nd, 2012; July 16th, 2013; July 3rd, 2014
Cooney	July 16th, 1998; July 19th, 1999; July 21st, 2000; July 24th, 2001; July 11th, 2002; July 16th, 2004; July 19th, 2005; July 22nd, 2006; July 25th, 2007; July 27th, 2008; July 30th, 2009; July 17th, 2010; July 4th, 2011; June 28th, 2012; July 9th, 2013; August 29th, 2014

LANDFIRE (www.landfire.gov) is a database of landcover, fire and fuels related GIS data that is modeled from Landsat images including spatial raster layers describing disturbances, vegetation, fuels, and topography. The existing vegetation type layer from LANDFIRE was used to remove areas that are classified as a vegetation type other than conifer forest. The LANDFIRE layer was based on imagery obtained prior to the occurrence of the 2003 fires of this study. The forest pixels remaining within the four fire perimeters comprised the analysis area.

The MTBS data for each fire included a severity raster created from satellite images taken pre-fire and one year post-fire (Table 3) and a perimeter shapefile. The severity raster is a classification of the dNBR image where the breakpoints for fire severity classes are selected according to Key and Benson (2006) with adjustments of approximately 5%. We combined Key and Benson's (2006) unburned-low and the increased greeness MTBS classes together and called the class unburned. The MTBS documentation clearly states that there

are limitations to these data (www.mtbs.gov). One of those limitations is a bias towards showing the fire effects on canopy level vegetation compared to surface level vegetation (Eidenshink et al. 2007). This bias can be a limitation when the objective is to quantify first-order fire effects such as the consumption of the surface fuels and understory vegetation.

Table 3. Images dates that MTBS used for severity classification.

MTBS Image Dates		
Fire Name	Pre-Fire Image Date	Post-Fire Image Date
Wedge Canyon	July 17th, 2002	July 14th, 2004
Robert	July 10th, 2002	July 15th, 2004
Black Mountain 2	July 10th, 2002	July 23rd, 2004
Cooney Ridge	July 10th, 2002	July 23rd, 2004

BARC severity rasters were used to characterize the initial assessment of fire severity (Table 4). We combined the BARC severity with the MTBS severity to produce a total of 16 possible classes containing two severity levels, one from each data set. The combination of these stems from the idea that the BARC map provides a representation of burned area and the MTBS map provides information about fire-caused mortality including initial post-fire regeneration and delayed mortality (Kolden et al. 2012).

Table 4. Images dates that BAER used in creation of BARC maps. A combination of Landsat, Spot, and Aster images were used for these classifications. The Wedge Canyon fire was a single image assessment.

BARC Image Dates		
Fire Name	Pre-Fire Image Dates	Post-Fire Image Dates
Wedge Canyon		August 10th, 2003 (SPOT)
Robert	August 3rd, 20003 (ASTER)	August 10th, 2003 (SPOT)
Black Mountain 2	July 10th, 2002 (LANDSAT)	September 31st, 2003 (SPOT)
Cooney Ridge	September 3rd, 2001 (SPOT)	August 31st, 2003 (LANDSAT)

From initial investigation we noticed trends in both the pre- and post-fire models for all the severity classes. We used the unburned class as a baseline trend and removed this trend from the burn severity models to show only the variability between classes caused by the difference in severity. The unburned class can contain areas that burned very lightly in small patches but typically these areas are completely unburned. In addition to the trend in NDVI recovery rate by severity class we also documented the mean NDVI for each year to show the variability from year to year.

To better understand the difference and similarities between the BARC and MTBS assessments and what occurred at each of the different severity levels and combinations of BARC and MTBS severity levels, we performed a visual interpretation of change in aerial imagery acquired pre-fire and post-fire. The pre-fire imagery was from the late 1980's to the early 1990's and were obtained from Montana Geographic Information Clearinghouse. Post-fire imagery were obtained from the National Agricultural Imagery Program (NAIP). Image interpretation was performed at 600 locations stratified along the MTBS/BARC classes. We

were particularly interested in points that showed a mismatch in severity level from BARC to MTBS, for example combinations such as high severity in BARC but unburned in MTBS, and vice versa.

Statistics

A stratified random sample of points was created across the 16 BARC/MTBS classes. NDVI values for each year during the time period 1998 – 2014 were extracted at these points, and linear models for NDVI versus time were generated for the unburned models first. Then these unburned models were subtracted from the other severity levels values. All other models were then created using the linear model list function from the Linear and Nonlinear Mixed Effects Models package in R (Pinheiro et al. 2015). All of the samples were plotted with NDVI on the y-axis and time in years relative to the fires on the x-axis. To determine when the NDVI within these classes returned to pre-fire NDVI, we show when the post-fire NDVI model crosses the pre-fire end point using a horizontal line of the lowest point of the pre-fire model. We applied a Z test using R (R Core Team 2014) to determine if the models of NDVI over time were significantly different between BARC/MTBS classes.

Results

NDVI recovery time within BARC and MTBS severity classes

To evaluate whether there was a difference in the time it takes for NDVI to return to pre-fire values we plotted NDVI versus time for the different fire severity levels using the BARC classification (Figure 2) and the MTBS classification (Figure 3). Full recovery in NDVI was achieved approximately 10 -35 years post-fire in mixed conifer forests of Montana. The

BARC severity classification show a much lower variation in the time to recover to pre-fire NDVI between severity classes compared to the MTBS classification. BARC shows recovery times with low takings 35 years, moderate at 24 years, and high taking 21 years (Figure 2). According to the extended assessment (MTBS), we observe differences in NDVI recovery time ranging from 10 to 13 years. A Z-test was performed to show that the models significantly differ from one another at the 0.05 significance level (Paternoster et al. 1998). The Z-test showed that the models of the NDVI recovery models were significantly different between severity classes for both the BARC and the MTBS classifications, indicating that NDVI increases at significantly different rates depending on the fire severity (Figure 4). To display these we used a graphic that compares the different classes within a severity metric and colors the cells black if they are significantly different and grey if they are not. This type of graph is typically called a heatmap.

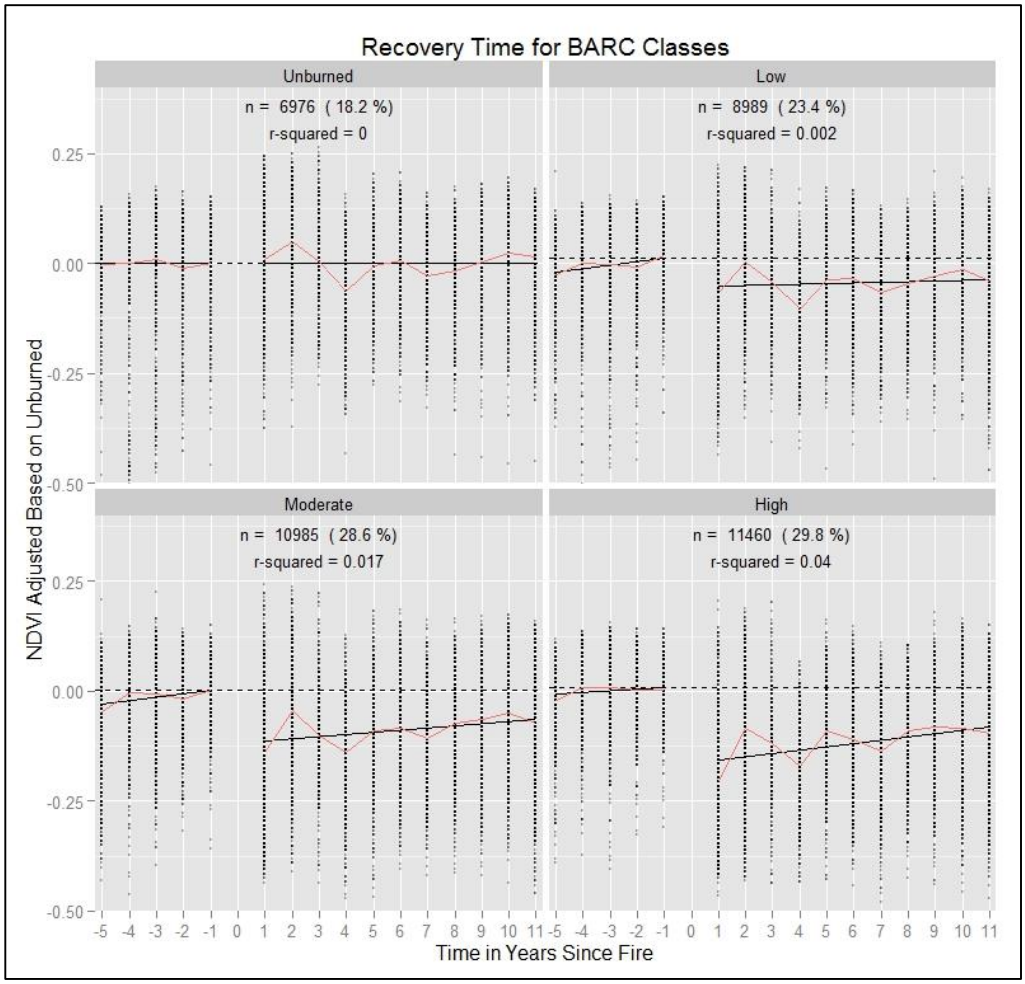

Figure 2. NDVI versus years since fire for each of the four BARC severity classes pre- and post-fire. Regression lines (solid) are included for both the pre-fire and the post-fire models. The dashed horizontal line shows the NDVI value of the model the year before the fire. The difference in NDVI recovery time from unburned to high severity was only about 14 years.

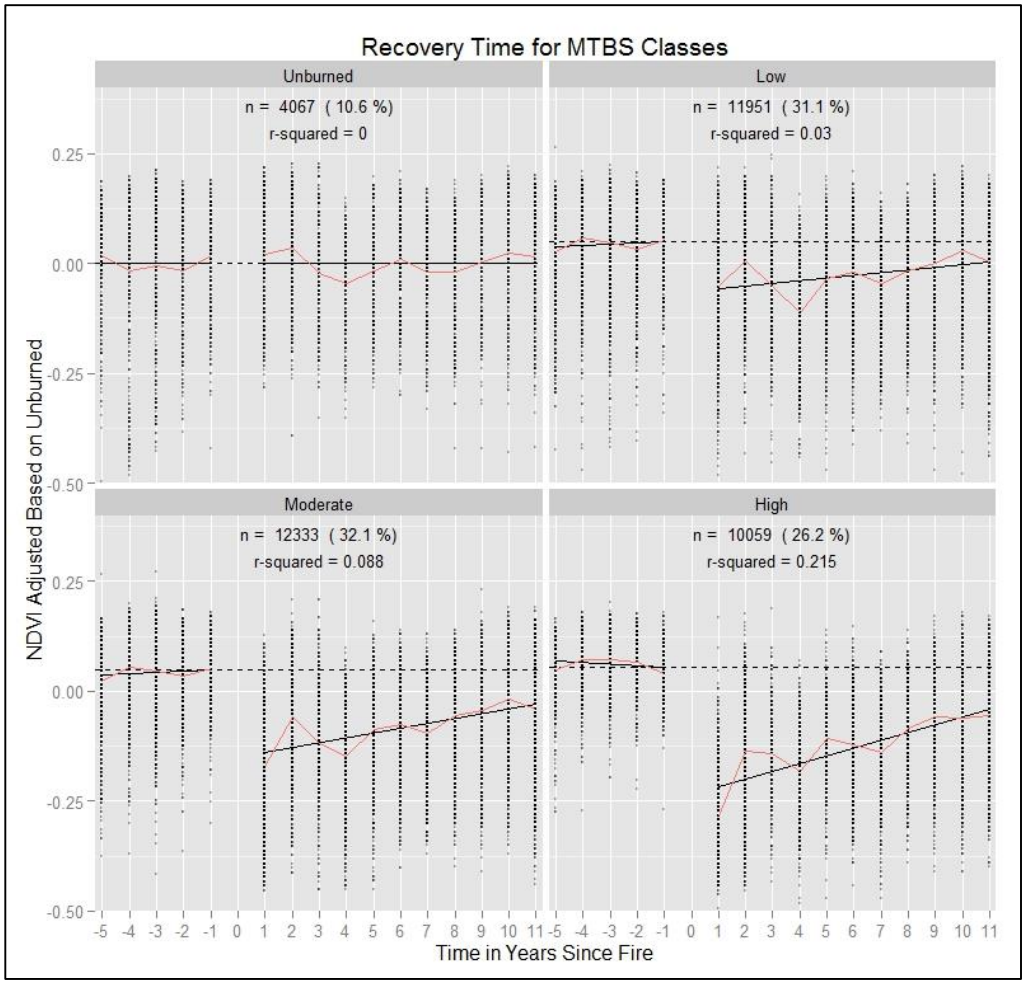

Figure 3. NDVI vs years since fire for each of the four MTBS severity classes pre-and post-fire. Regression lines (solid) are included for both the pre-fire and the post-fire data models. The dashed horizontal line shows the NDVI value the year before the fire, which was the lowest NDVI observed prior to the fire. There was an increase in NDVI recovery time from unburned to high severity of about 3 years.

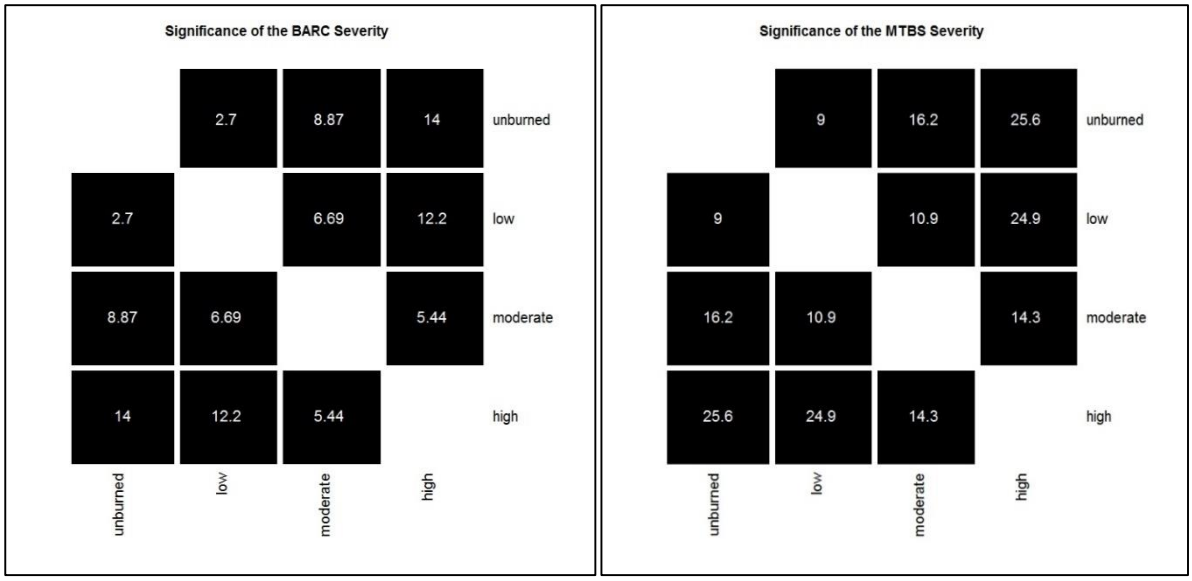

Figure 4. These heatmaps show which severity class recovery models were significantly different from each other for the BARC (left) and MTBS (right) classifications. The white cells are those that are not significantly different from one another and the black cells are significantly different from one another. All classes were significantly different from one another but it is important to note that the MTBS severity is more significantly different than the BARC severity classes are. The numbers in the cells represent the z-scores.

Recovery Time for the Combined BARC and MTBS severity classes

To better understand the spatial context and extents of the combinations of BARC/MTBS classes we created a map of the combinations (Figure 5). A large portion of the Wedge Canyon and Robert fires have no data there was no BARC classification available for the area.

Black Mountain 2 Change in Severity Classes

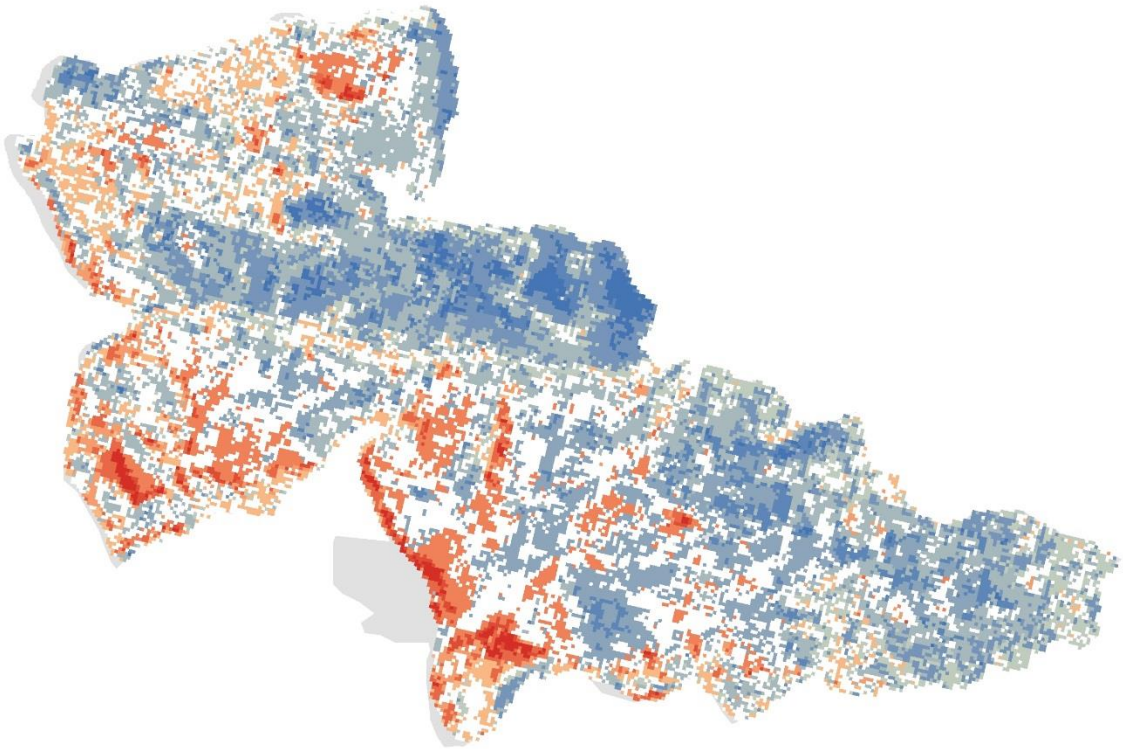

WGS 1984 UTM Z11 N
By: Kevin Satterberg
Data provided by:
BARC and MTBS

0 0.5 1 2
Kilometers

Combined Severity Classes With Percent Area

BARC-MTBS

- High-Unburned (1.9%)
- High-Low (4.1%)
- Moderate-Unburned (9.7%)
- High-Moderate (9.3%)
- Moderate-Low (18.2%)
- Low-Unburned (6.2%)
- No Change (High 5.31%)
- No Change (Moderate 13.6%)
- No Change (Low 10.6%)
- No Change (Unburned 3.9%)
- Unburned-Low (5.5%)
- Low-Unburned (2.8%)
- Moderate-High (5.7%)
- Unburned-Moderate (1.8%)
- Low-High (0.8%)
- Unburned-High (0.7%)
- No Data

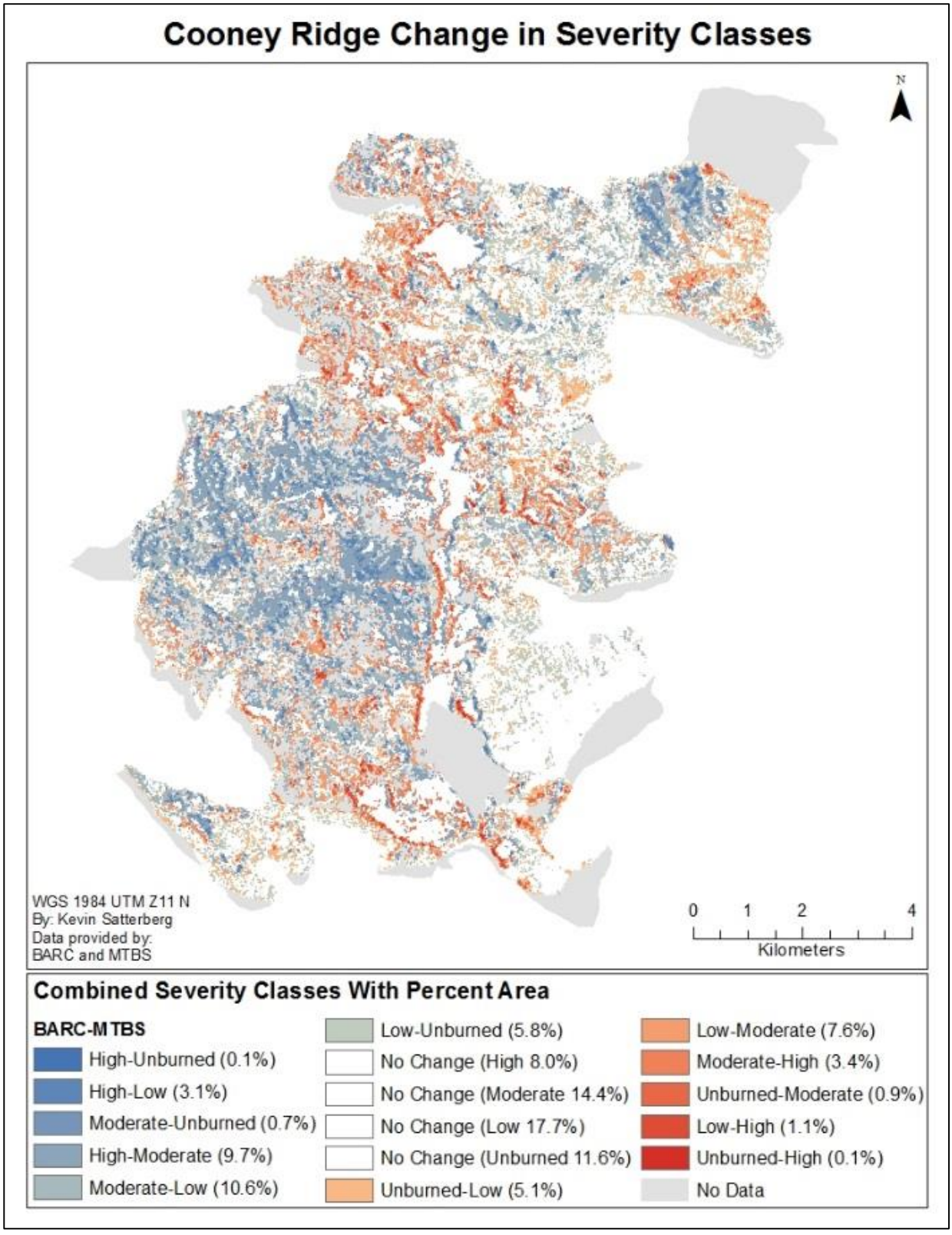
Cooney Ridge Change in Severity Classes
N
WGS 1984 UTM Z11 N
By: Kevin Satterberg
Data provided by:
BARC and MTBS
0 1 2 4
Kilometers
Combined Severity Classes With Percent Area
BARC-MTBS
High-Unburned (0.1%)
High-Low (3.1%)
Moderate-Unburned (0.7%)
High-Moderate (9.7%)
Moderate-Low (10.6%)
Low-Unburned (5.8%)
No Change (High 8.0%)
No Change (Moderate 14.4%)
No Change (Low 17.7%)
No Change (Unburned 11.6%)
Unburned-Low (5.1%)
Low-Moderate (7.6%)
Moderate-High (3.4%)
Unburned-Moderate (0.9%)
Low-High (1.1%)
Unburned-High (0.1%)
No Data

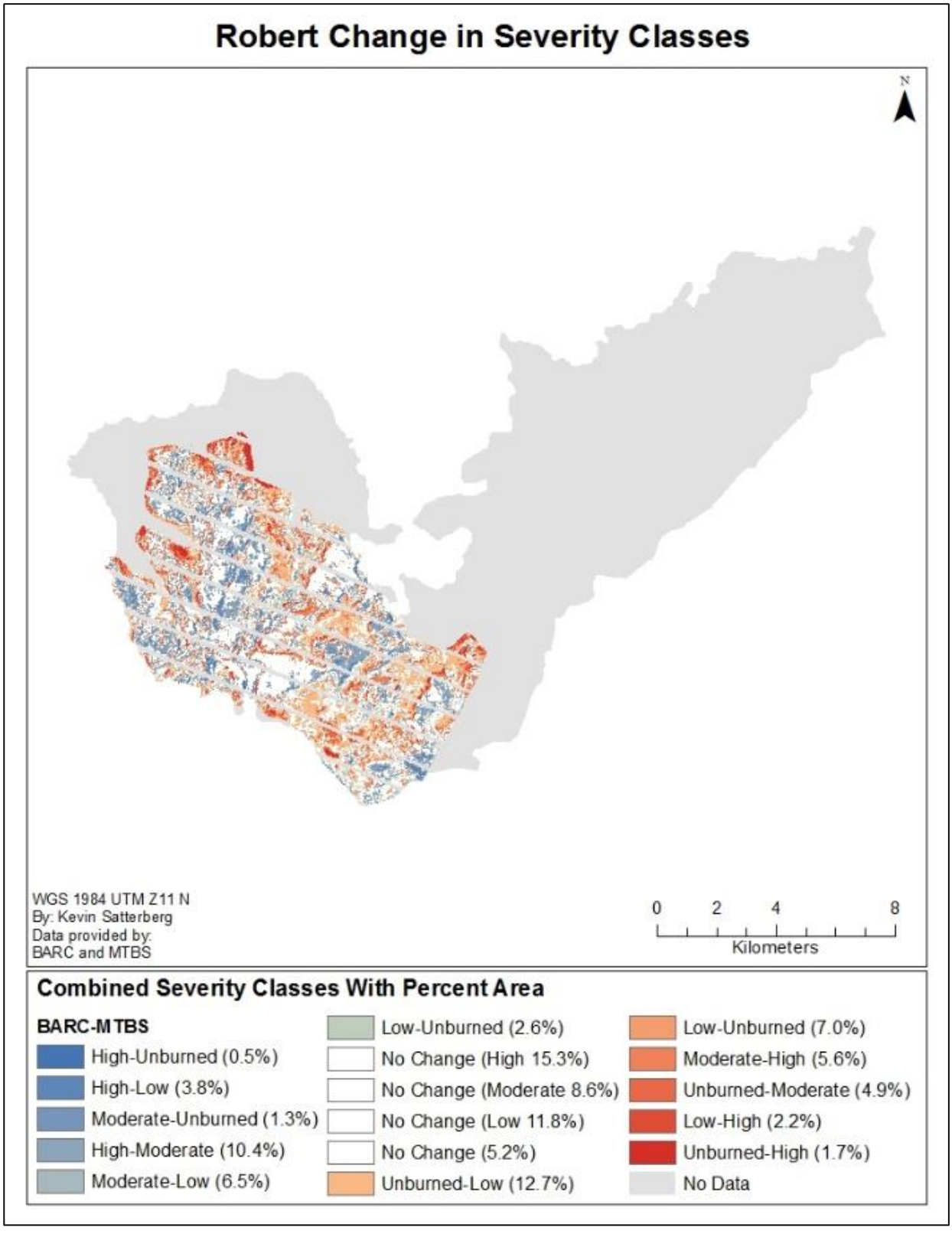
Robert Change in Severity Classes
N
WGS 1984 UTM Z11 N
By: Kevin Satterberg
Data provided by:
BARC and MTBS
0 2 4 8
Kilometers
Combined Severity Classes With Percent Area
BARC-MTBS
High-Unburned (0.5%)
High-Low (3.8%)
Moderate-Unburned (1.3%)
High-Moderate (10.4%)
Moderate-Low (6.5%)
Low-Unburned (2.6%)
No Change (High 15.3%)
No Change (Moderate 8.6%)
No Change (Low 11.8%)
No Change (5.2%)
Unburned-Low (12.7%)
Low-Unburned (7.0%)
Moderate-High (5.6%)
Unburned-Moderate (4.9%)
Low-High (2.2%)
Unburned-High (1.7%)
No Data

Wedge Canyon Change in Severity Classes

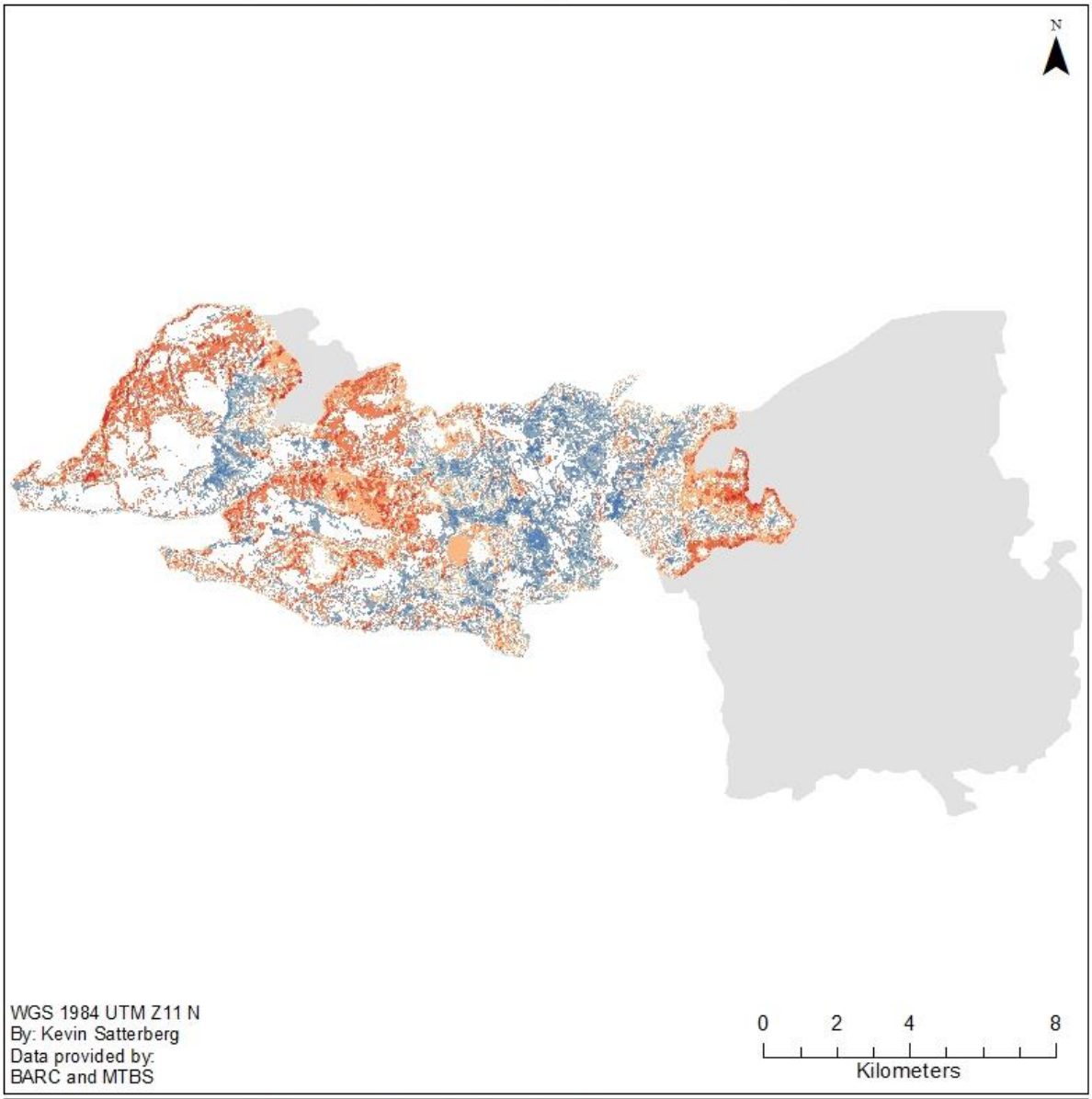

Combined Severity Classes With Percent Area

BARC-MTBS

- High-Unburned (0.4%)
- High-Low (3.6%)
- Moderate-Unburned (1.1%)
- High-Moderate (9.6%)
- Moderate-Low (7.4%)
- Low-Unburned (1.8%)
- No Change (High 22.7%)
- No Change (Moderate 10.2%)
- No Change (Low 7.9%)
- No Change (Unburned 4.8%)
- Unburned-Low (8.2%)
- Low-Moderate (6.7%)
- Moderate-High (8.8%)
- Unburned-Moderate (3.9%)
- Low-High (2.2%)
- Unburned-High (0.7%)
- No Data

Figure 5. The above maps show the combination of the severity classifications with BARC being the first severity classification and MTBS being the second in each of the classes displayed in the legend. The areas with no change are white and those that changed are either a red or blue hue. The blue hues represent areas where BARC is a higher severity than MTBS and red represents the opposite. The larger the difference in severity levels the dark the color. The percentage following the combined class name is the percentage of the area that class encompasses.

We further plotted NDVI values against time since fire for all BARC/MTBS combinations (Figure 6). The dashed horizontal line represents the end point of the pre-fire model and was included as a guide showing when the post-fire model returned to pre-fire NDVI values. The post-fire models all increase in NDVI over time and cross the horizontal line at different times depending on the combination of BARC and MTBS severity (Figure 6). The MTBS low severity class show the greatest variability where returning to pre-fire NDVI takes five to 15 years depending on the associated BARC severity level. The MTBS moderate severity class shows similar variability with a return to pre-fire NDVI taking eight to 17 years depending on the associated BARC severity level. The moderate and high MTBS classes show more consistency with only a few years between the different MTBS classes. The unburned BARC severity classification shows the highest range (5-10years) in the time it takes to return to pre-fire NDVI. The high BARC severity shows the most consistency with recovery time with a range of only three years difference between classes to return to pre-fire NDVI. The combination of BARC high and MTBS unburned severity has a low sample size compared to the other combinations with only 47 samples.

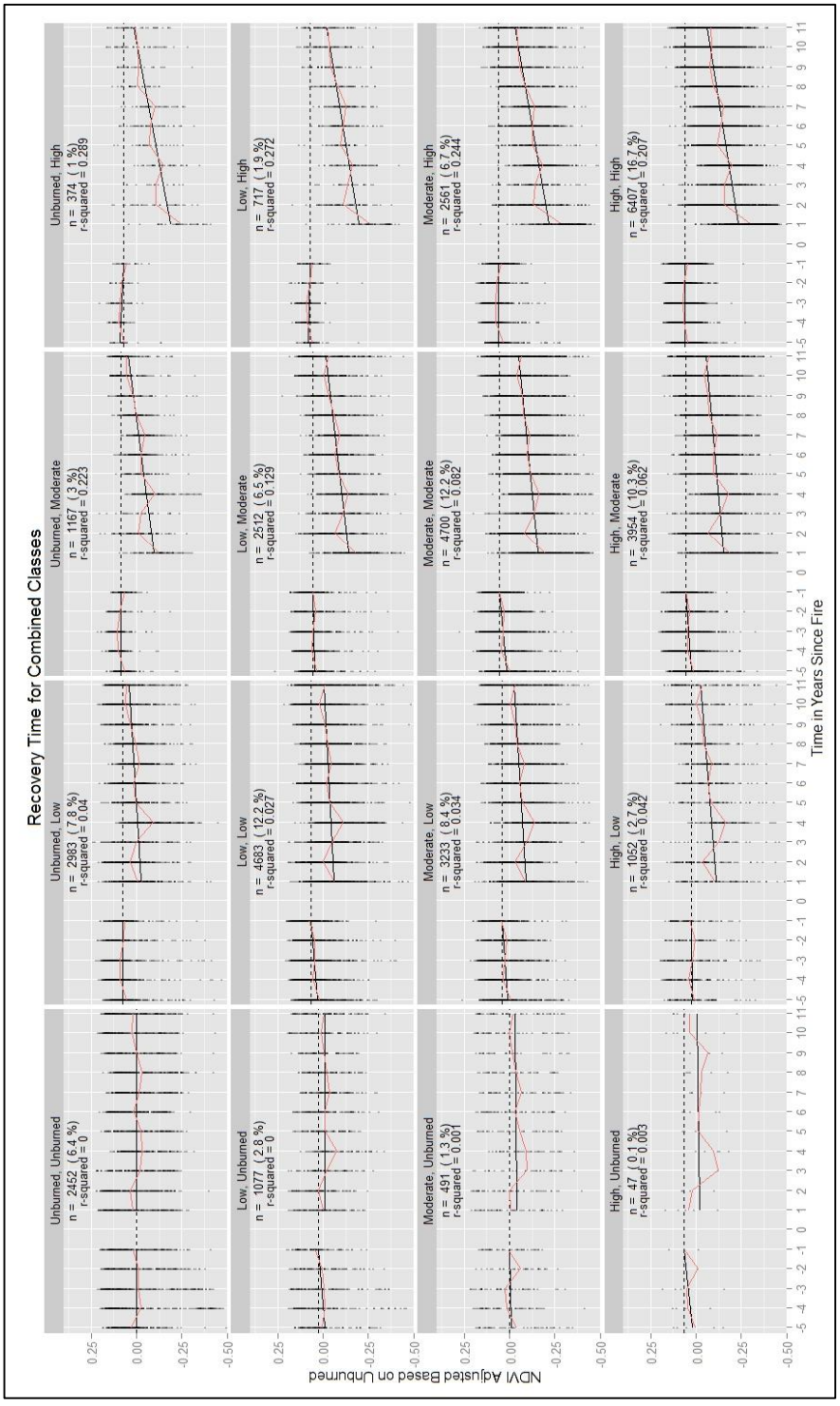

Figure 6. Plot of all the NDVI recovery models for randomly selected pixels within combinations of BARC/MTBS classes ranging from unburned to high severity.

To understand how these NDVI chronosequences of BARC/MTBS combinations differ from each other, we tested the models using a Z-test of significance for large sample sizes at the 0.05 significance level (Paternoster et al. 1998).

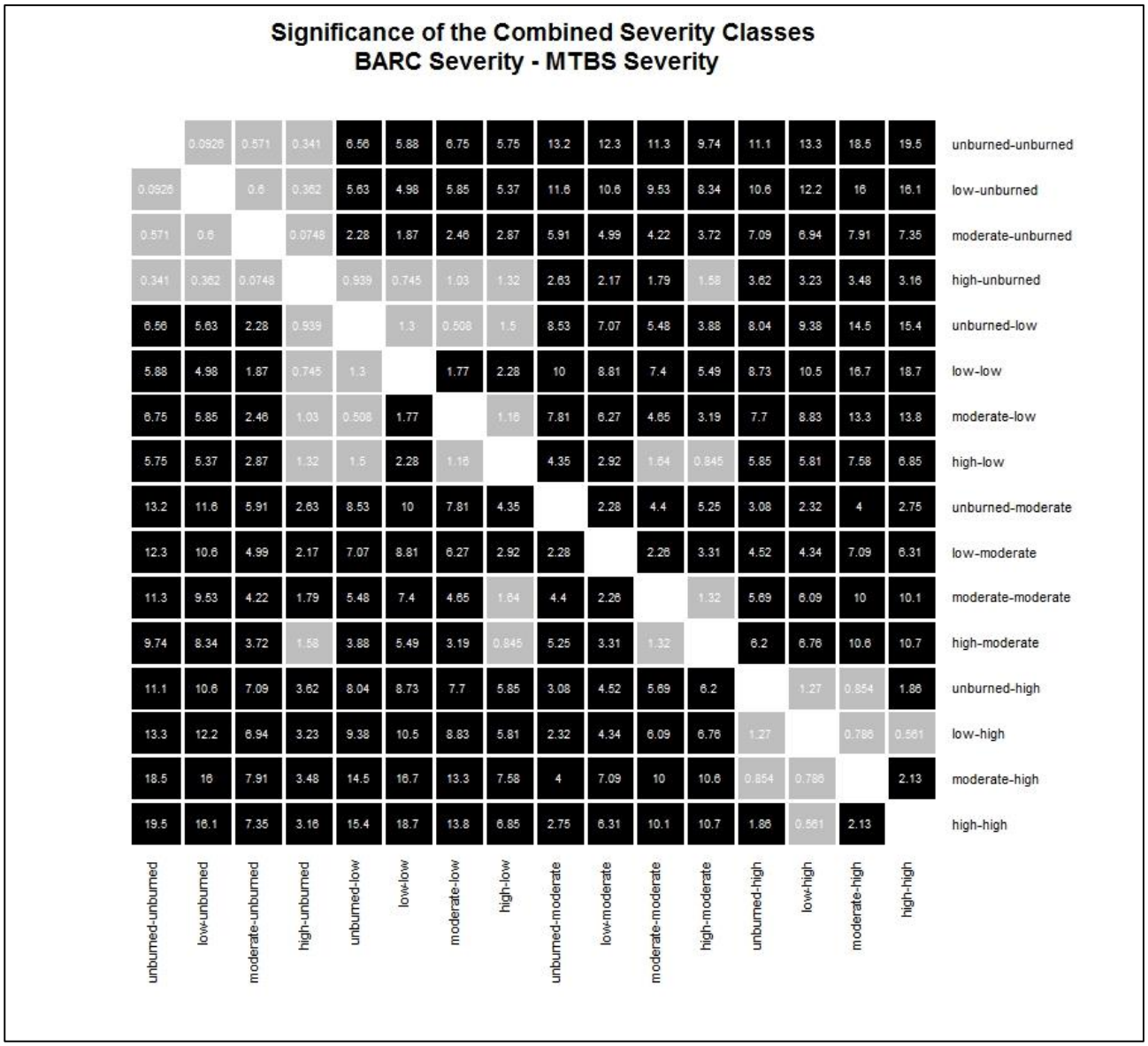

Figure 7. This is a heat map showing what combinations of BARC/MTBS severity were significantly different from one another. The format for the labels is: BARC severity – MTBS

severity. The black cells are significantly different from one another (alpha = 0.05) where the grey cells are not. The number in the cell represents the Z-scores.

The heat map (Figure 7) shows black cells for where the recovery models of NDVI were significantly different from each other. The grey cells represent combinations that were not significantly different from one another. The upper right and the lower left are divided by empty cells because those are where the slopes are exactly the same, meaning that the upper right and lower left are mirror images of one another. Combinations along the center line tend to be non-significant. Combinations that include the unburned MTBS severity are also not significantly different from other combinations with MTBS unburned severity. The same is observed for MTBS low severity with low-low being the only exception. The combinations that include a high severity component tend to be significantly different from combinations that include an unburned or low severity component.

Aerial Photograph Interpretation of outlying groups

To better understand how the forest recovered after the wildfire and the relationship between recovery and remotely sensed severity measures we looked at aerial photos acquired pre- and post-fire. Photos were provided by the Montana State GIS clearinghouse (black & white) and NAIP (color photos). There were a few limitations with the data from Montana because of the remote nature of the northwestern wildfires. All of the aerial photos were 1-m resolution, but some of the pre-fire images for the northern wildfires were acquired in the 80's. No wildfire occurred between the time of the pre-fire images and the

wildfires being studied. Harvesting practices or weather damage could have occurred during the time after the pre-fire images and before the fire resulting in some error.

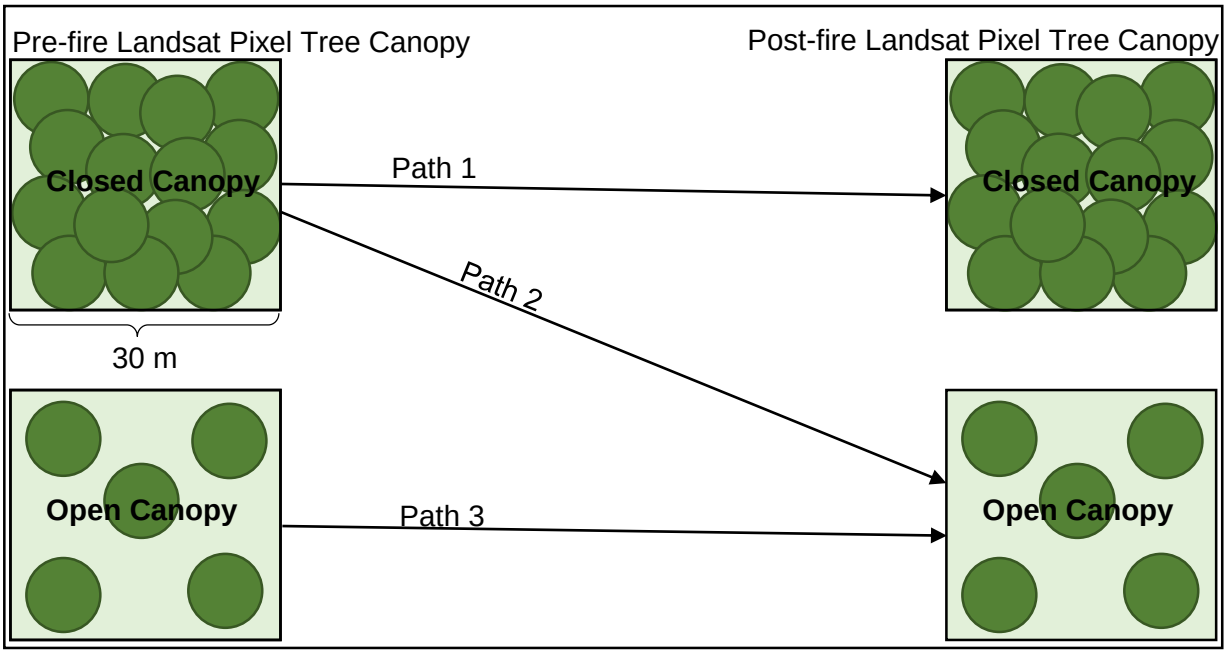

BARC, MTBS (n)	Path 1	Path 2	Path 3
Unburned,Unburned (10)	20%	0%	80%
Unburned,Low (10)	20%	10%	70%
Unburned,Moderate (10)	10%	50%	40%
Unburned,High (10)	0%	90%	10%
Low,Unburned (10)	0%	10%	90%
Low,Low (10)	30%	10%	60%
Low,Moderate (10)	10%	30%	60%
Low,High (10)	0%	90%	10%
Moderate,Unburned (10)	10%	20%	70%
Moderate,Low (10)	10%	0%	90%
Moderate,Moderate (10)	10%	40%	50%
Moderate,High (10)	0%	60%	40%
High,Unburned (3)	0%	0%	100%
High,Low (10)	0%	10%	90%
High,Moderate (10)	0%	40%	60%
High,High (10)	0%	90%	10%

Figure 8. This figure shows a representation of the change we observed in aerial photos due to a wildfire. The green circles within the squares represent trees within a Landsat pixel. The table shows the percentage of each class combination that followed that path due to a wildfire.

Based on the information in Figure 8 it is apparent that when BARC records a higher severity than MTBS, path 3 is the dominate path, i.e. forests with an open canopy both before and after the fire. When MTBS severity is higher than BARC the forest often follows path 2, going from a closed canopy pre-fire to an open canopy post-fire, but there are times that we see these severity combinations following path 3. When the difference in severity between BARC and MTBS is large, path 3 is the dominating path. The high (BARC), unburned (MTBS) combination had a lower sample size because the combination only covers 0.1% of the area (Figure 6). These areas are typically only a few pixels and surrounded by other combinations where BARC is higher than MTBS.

Discussion

NDVI recovery time for BARC and MTBS severity classes

Overall the recovery time within severity classes of both severity metrics (BARC and MTBS) is in agreement with previous research. Hicke et al. (2003) show that Net Primary Productivity (NPP) in North American boreal forests has returned to pre-fire levels nine years following the fire based on remote sensing assessments that were performed using the Moderate Resolution Imaging Spectroradiometer (MODIS). It is important to note that NPP does not show the change in vegetation type from trees to shrub or herbaceous vegetation,

similar to NDVI derived from Landsat images. The aerial photo analysis is therefore essential to understand the shift in vegetation type and structure. The MTBS severity classes show a lower range of recovery times (3 years) while BARC has a much larger range (14 years). This was also observed in the heatmaps showing that the Z-statistics are much higher for MTBS severity classes compared to BARC severity classes (Figure 4). This could be expected because the MTBS severity metric focuses on delayed mortality and initial recovery (Key & Benson 2006) while BARC severity maps include areas where the above-ground understory vegetation has been blackened but not necessarily incurred mortality.

Recovery time for the combined BARC and MTBS severity classes

Severity maps produced by MTBS and BAER are readily available and have plenty of supporting documentation on how to use the data effectively. Many times only one of these data sets is used in land management or research. When combining the two we generate additional information on how much vegetation was burned and initial vegetation recovery (Key & Benson 2006).

In 25.6% of the samples, the severity from the BARC assessment was higher than the severity observed in the MTBS assessment. The photo interpretation indicates that that these areas represent the scenario where no change occurred in the tree canopy cover, however herbaceous, shrub, or grass canopy in the interspaces between trees incurred mortality due to the fire. Herbaceous and shrub vegetation recover much quicker than trees so when the post-fire image is taken for MTBS these areas are already approaching pre-fire greenness.

In the majority of the area where BARC showed unburned pixels and MTBS showed moderate to high severity pixels, we suggest there was damage or consumption of tree crowns, resulting in prolonged recovery times. When this is reversed and BARC is higher than MTBS we see much more variability in recovery times. When MTBS is unburned there is little to no recovery time, except when BARC is high then there is a longer recovery time but a low sample size to confound the results. When we look at the four graphs when the severity class is the same for BARC and MTBS we see a steady increase in recovery time from unburned to high, as expected. The high-unburned group lacked a high sample size so most of the time it was not significantly different than other combinations. To better understand whether a species or vegetation type shift occurred, for examples from shrubs to grasses, we need higher resolution images and possibly field work to validate the image results.

Aerial Photograph interpretation of outlying groups

Aerial photo interpretation provided information regarding the changes in vegetation structure that occurred as a result of the wildfire, complementary to the spectral reflectance changes observed via Landsat. The first set of combinations, when there is no difference between BARC and MTBS, i.e. they both show low, moderate, or high severity covers 47.5% of the analysis area. Within these combinations, we suggest that there will be a gradient of time to recovery with low severity being the shortest and high severity being the longest. The low severity locations will have little to no damage to the trees and were likely caused by a surface fire, thus the only vegetation type that is recovering would be grasses, forbs, shrubs, and small trees. The high severity areas show damage to the tree canopy as well as the understory vegetation. In places where BARC shows a higher severity class than MTBS,

we expect to see damage or removal of the tree canopy and quick green up of the grasses or limited canopy and large density of shrubs, grasses, and forbs. When MTBS severity is higher than BARC, we expect to see some of the tree canopy remaining, but removal of a majority of the grasses, forbs, and shrubs. It is important to note that when MTBS is higher than BARC we could also see more canopy damage in the form of discoloration which later leads to mortality, snags or downed trees. It is important to note that one pixel can contain one or more of the fire types, effects, and severities (Kolden et al. 2012), particularly in the moderate and low severity pixels.

When looking at high BARC severity samples, MTBS increases while there is a shift from the majority of samples following path 2 to path 3. We believe this is due to BARC detecting more char in the background, which may lead to misclassification of the remaining green vegetation. This misclassification could be due to the fact that char no longer has leaves with water in the leaf cells. The NIR band used in the calculation of NBR is directly connected to leaf cell water content (Tucker 1979). The MTBS post-fire image is taken a year after the fire when some of the ground vegetation has returned resulting in more visible leaf cell water content than that of the BARC post fire image.

The aerial photos show the loss in tree canopy but are not high enough in spatial resolution to show individual understory species, so therefore an assessment of understory species shifts from aerial photos is not possible. The pre-fire aerial imagery were also black-and- white making it impossible to see discolored trees pre-fire, thus it was impossible to see trees had been heavily damaged. From Landsat a single tree canopy cannot be seen and if an

area of tree crowns were not destroyed but damaged, resulting in a live tree that will simply take longer to recover compared to shrubs and herbaceous vegetation.

On the opposite side of the severity spectrum; areas that showed low severity, or were classified as unburned in the BARC assessment, but were classified in a higher severity class in the MTBS assessment, may be a sign of delayed mortality post-fire. This could also be an effect of the lower amount of charred debris in the MTBS image compared to BARC, thus no large difference in the NIR band and leaf cell water content. These areas potentially had larger fuel loads of coarse woody debris (logs) or deep duff that were able to smolder for long periods of time resulting in tree mortality and damage to the soil, below ground vegetative structures and the seedbank (Ryan 2002; Stephan et al. 2010). Trees killed from delayed mortality within a year of the fire would contribute to a higher severity classification in the MTBS compared to the BARC assessment.

Conclusion and management implications

Based on aerial photo interpretation and overlays with the freely available BARC and MTBS severity products we conclude that the MTBS product provides better understanding of the long term effects of wildfires in mixed conifer forests. This research has shown interesting results some of which were unexpected. The BARC and MTBS severity products often show different results, in fact, they were in agreement only in 47.5% of the analysis area. When combined, we can better understand wildfire effects on the area. When BARC shows considerably higher severity than MTBS, the area is likely composed of open forest pre-fire and the initially observed high severity represents removal of understory shrubs and herbaceous vegetation as well as a pixel saturated by charred debris. When MTBS shows

considerably higher severity than BARC the area has likely incurred high tree mortality. Overall this process was meant to be simple so that any agency that has access to GIS software can process the free BARC and MTBS data and better focus rehabilitation efforts. This methodology can help managers to prioritize post-fire assessments and treatments in the forested areas in the most urgent need of rehabilitation.

References

Arno, S. F. (1980). Forest fire history in the northern Rockies. *Journal of Forestry*, *78*, 460–465.

Brewer, C. K., Winne, J. C., Redmond, R. L., Opitz, D. W., & Mangrich, M. V. (2005). Classifying and Mapping Wildfire Severity: A Comparison of Methods. *Photogrammetric Engineering & Remote Sensing*, *71*(11), 1311–1320.

Cooper, S. V., Neiman, K. E., & Roberts, D. W. (1991). *Forest habitat types of northern Idaho: a second approximation*. Odgen, UT. Retrieved from http://www.fs.fed.us/rm/pubs_int/int_gtr236.pdf

Eidenshink, J., Schwind, B., Brewer, K., Zhu, Z.-L., Quayle, B., & Howard, S. (2007). A project for Monitoring Trends in Burn Severity. *Fire Ecology*, *3*(1), 3–21.

Hayes, J. J., & Robeson, S. M. (2013). Spatial Variability of Landscape Pattern Change Following a Ponderosa Pine Wildfire in Northeastern New Mexico, USA. Retrieved from http://www.tandfonline.com/doi/abs/10.2747/0272-3646.30.5.410

Hicke, J. A., Asner, G. P., Kasischke, E. S., French, N. H. F., Randerson, J. T., James Collatz, G., … Field, C. B. (2003). Postfire response of North American boreal forest net primary productivity analyzed with satellite observations. *Global Change Biology*, *9*(8), 1145–1157. http://doi.org/10.1046/j.1365-2486.2003.00658.x

Hoff, V., Teske, C. C., Riddering, J. P., Queen, L. P., Gdula, E. G., & Bunn, W. A. (2014). Changes in severity distribution after subsequent fires on the North Rim of Grand Canyon National Park, Arizona, USA. *Fire Ecology*, *10*(2), 48–63.

Hudak, A. T., Penelope, M., Bobbitt, M. J., Smith, A. M. S., Lewis, S. A., Lentile, L. B., … McKinley, R. A. (2007). The relationship of multispectral satellite imagery to immediate fire effects. *Fire Ecology*, *3*(1), 64–90.

Key, C. H., & Benson, N. C. (2006). *Landscape assessment: ground measure of severity, the Composite Burn Index, and remote sensing of severity, the Normalized Burn Ratio. FIREMON: Fire Effects Monitoring and Inventory System. Gen. Tech. Rep. RMRS-GTR-164-CD* (Vol. USDA Fores). Ogden, UT: USDA Forest Service, Rocky Mountain Research Station: LA 1–51.

Kolden, C. A., Lutz, J. A., Key, C. H., Kane, J. T., & van Wagtendonk, J. W. (2012). Mapped versus actual burned area within wildfire perimeters: Characterizing the unburned. *Forest Ecology and Management*, *286*(0), 38–47. http://doi.org/http://dx.doi.org/10.1016/j.foreco.2012.08.020

Lannom, K.O., Smith, A.M.S., Tinkham, W.T., Satterberg, K., and Strand, E.K. Development of an extreme wildland fire recovery chronosequence. Remote Sensing Letters, in review.

Lentile, L. B., Morgan, P., Hudak, A. T., Bobbitt, M. J., Lewis, S. A., Smith, A. M. S., & Robichaud, P. R. (2007). Post-fire burn severity and vegetation response following eight large wildfires across the Western United States. *Fire Ecology*, *3*(1), 91–108. Retrieved from http://www.treesearch.fs.fed.us/pubs/29509

M.J., L. G., & Caselles, V. (1991). Mapping burns and natural reforestation using thematic Mapper data. *Geocarto International*, *6*(1), 31–37.

Masek, J. G., Vermote, E. F., Saleous, N. E., Wolfe, R., Hall, F. G., Huemmrich, K. F., … Teng-Kui, L. (2006). A Landsat surface reflectance dataset for North America, 1990-2000.

Geoscience and Remote Sensing Letters, IEEE, *3*(1), 68–72. http://doi.org/10.1109/lgrs.2005.857030

Morgan, P., Keane, R. E., Dillon, G. K., Jain, T. B., Hudak, A. T., Karau, E. C., … Strand, E. K. (2014). Challenges of assessing fire and burn severity using field measures, remote sensing and modelling. *International Journal of Wildland Fire*, *23*(8), 1045. http://doi.org/10.1071/WF13058

Myneni, R. B., Hall, F. G., Sellers, P. J., & Marshak, A. L. (1995). The interpretation of spectral vegetation indexes. *IEEE Transactions on Geoscience and Remote Sensing*, *33*(2), 481–486. http://doi.org/10.1109/36.377948

National Interagency Fire Center, F. F. and A. T. G. (2015). *2015 Interagency Standards for Fire and Fire Aviation*. Boise, Idaho: National Interagency Fire Center.

Paternoster, R., Brame, R., Mazerolle, P., & Piquero, A. (1998). USING THE CORRECT STATISTICAL TEST FOR THE EQUALITY OF REGRESSION COEFFICIENTS. *Criminology*, *36*(4), 859–866. http://doi.org/10.1111/j.1745-9125.1998.tb01268.x

Pfister, R. D., Kovalchik, B. L., Arno, S. F., & Presby, R. C. (1977). *Forest habitat types of Montana.* Ogden, Utah: US Department of Agriculture, Forest Service, Intermountain Forest and Range Experiment Station. Retrieved from http://www.fs.fed.us/rm/pubs/rmrs_gtr292/1980_arno.pdf

Pinheiro, J., Bates, D., DebRoy, S., Sarkar, D., & Team, R. C. (2015). nlme: Linear and Nonlinear Mixed Effects Models.

Pyne, S. J. (1996). *Introduction to Wildland Fire* (2nd ed.). Hoboken, NJ: John Wiley & Sons, Incorporated.

R Core Team (2014). R: A language and environment for statistical computing. R Foundation for Statistical Computing, Vienna, Austria. URL http://www.R-project.org/.

Rehfeldt, G. L. (2006). *A spline model of climate for the Western United States.* Fort Collins, CO. URL http://forest.moscowfsl.wsu.edu/climate/customData/.

Reinhardt, E. D., Keane, R. E., & Brown, J. K. (1997). *First Order Fire Effects Model: FOFEM 4.0, user's guide*. Ogden, UT.

Ryan, K. C. (2002). Dynamic Interactions between Forest Structure and Fire Behavior in Boreal Ecosystems. *Silva Fennica*, *36*(1), 13–39.

Scott, J. H., & Burgan, R. E. (2005). *Standard Fire Behavior Fuel Models : A Comprehensive Set for Use with Rothermel ' s Surface Fire Spread Model*. *Natural Resources Research* (Vol. RMRS-GTR-1). Fort Collins, CO. Retrieved from http://pyrologix.com/ScottBurgan2005-GTR-153.pdf

Seavy, N. E., & Alexander, J. D. (2014). Songbird response to wildfire in mixed-conifer forest in south-western Oregon. *International Journal of Wildland Fire*, *23*(2), 246–258. http://doi.org/10.1071/wf12081

Smith, A.M. S., Eitel, J.U. H. & Hudak, A.T., 2010. Spectral analysis of charcoal on soils: implications for wildland fire severity mapping methods. *International Journal of Wildland Fire,* 19(7), p. 976-983.

Smith, J. K., & Fischer, W. C. (1997). *Fire ecology of the forest habitat types of northern Idaho*. Ogden, Utah.

Solomon, S., Qin, D., Manning, M., Chen, Z., Marquis, M., Averyt, K. B., … Tignor, M. (2007). *IPCC, 2007: Climate Change 2007: The Physical Science Basis. Contribution of Working*

Group I to the Fourth Assessment Report of the Intergovernmental Panel on Climate Change. Cambridge, United Kingdom and New York, NY, USA.

Stein, S. M., Menakis, J., Carr, M. A., Comans, S. J., Stewart, S. I., Cleveland, H., … Radeloff, V. C. (2013). *Wildfire, wildlands, and people: understanding and preparing for wildfire in the wildland-urban interface-a Forests on the Edge report.* Fort Collins.

Stephan, K., M., M., & Dickinson, M. B. (2010). First-order fire effects on herbs and shrubs: present knowledge and modeling needs. *Fire Ecology*, *6*(1), 95–114.

Strand, E. K., Bunting, S. C., & Keefe, R. F. (2013). Influence of Wildland Fire Along a Successional Gradient in Sagebrush Steppe and Western Juniper Woodlands. *Rangeland Ecology & Management*, *66*(6), 667–679. http://doi.org/10.2111/REM-D-13-00051.1

Tucker, C. J. (1979). Red and photographic infrared linear combinations for monitoring vegetation. *Remote Sensing of Environment*, *8*(2), 127–150. http://doi.org/10.1016/0034-4257(79)90013-0

Vierling, K. T., Lentile, L. B., & Nielsen-Pincus, N. (2008). Preburn Characteristics and Woodpecker Use of Burned Coniferous Forests. *The Journal of Wildlife Management*, *72*(2), 422–427. http://doi.org/10.2193/2006-212

Westerling, A. L., Hidalgo, H. G., Cayan, D. R., & Swetnam, T. W. (2006). Warming and Earlier Spring Increase Western U.S. Forest Wildfire Activity. *Science*, *313*(5789), 940–943. http://doi.org/10.1126/science.1128834

Appendix 1.

List of all the species and their lifeforms that were found during the 2013 and 2014 field work.

FORM	CODE	SCIENTIFIC NAME	COMMON NAME
TREE	ABGR	Abies grandis	Grand fir
TREE	ABLA	Abies lasiocarpa	Subalpine fir
TREE	LAOC	Larix occidentalis	Western larch
TREE	PIEN	Picea engelmannii	Engelmann spruce
TREE	PICO	Pinus contorta	Lodgepole pine
TREE	POTR	Populus tremuloides	Quaking aspen
TREE	PSME	Pseudotsuga menziesii	Douglas-fir
TREE	THPL	Thuja plicata	Western red cedar
SHRB	ACGL	Acer glabrum	Rocky Mountain maple
SHRB	ALSI	Alnus sinuata	Sitka alder
SHRB	AMAL	Amelanchier alnifolia	Serviceberry
SHRB	ARUV	Arctostaphylos uva-ursi	Kinnikinnick, bearberry
SHRB	BERE	Berberis repens	Creeping Oregon grape
SHRB	CESA	Ceanothus sanguineus	Redstem ceanothus
SHRB	CEVE	Ceanothus velutinus	Shinyleaf ceanothus
SHRB	CHUM	Chimaphila umbellata	Western pipsissewa
SHRB	HODI	Holodiscus discolor	Ocean-spray
SHRB	LIBO2	Linnaea borealis	Twinflower
SHRB	LOUT2	Lonicera utahensis	Utah honeysuckle
SHRB	MEFE	Menziesia ferruginea	Fool's huckleberry
SHRB	PAMY	Pachystima myrsinites	Myrtle boxwood
SHRB	PHMA	Physocarpus malvaceus	Ninebark
SHRB	RILA	Ribes lacustre	Prickly currant
SHRB	RIVI	Ribes viscosissimum	Sticky currant
SHRB	ROSA	Rosa sp.	Rose
SHRB	RUID	Rubus idaeus	Red raspberry
SHRB	RUPA	Rubus parviflorus	Western thimbleberry
SHRB	SALX	Salix sp.	Willow species
SHRB	SARA	Sambucus racemosa	Elderberry
SHRB	SHCA	Shepherdia canadensis	Buffaloberry
SHRB	SOSC2	Sorbus scopulina	Mountain-ash
SHRB	SOSI	Sorbus sitchensis	Sitka mountain-ash
SHRB	SPBE	Spiraea betulifolia	Spiraea
SHRB	SYAL	Symphoricarpos albus	Common snowberry
SHRB	SYOR	Symphoricarpos oreophilus	Mountain snowberry
SHRB	VAGL	Vaccinium globulare	Huckleberry

SHRB	VASC	Vaccinium scoparium	Grouse whortleberry
FORB	ACMI	Achillea millefolium	Common yarrow
FORB	ADBI	Adenocaulon bicolor	Pathfinder
FORB	AGSP	Agoseris sp.	Agoseris
FORB	ANMA	Anaphalis margaritacea	Pearly everlasting
FORB	ANMI	Antennaria microphylla	Rosy pussytoes
FORB	ANRA	Antennaria racemosa	Racemose pussytoes
FORB	APAN	Apocynum androsaemifolium	Spreading dogbane
FORB	AQFL	Aquilegia flavescens	Yellow columbine
FORB	ARCO	Arnica cordifolia	Heartleaf arnica
FORB	ARNU	Aralia nudicaulis	Wild sarsaparilla
FORB	ARSP	Arabis sp.	Rockcress
FORB	ASCO	Aster conspicuus	Showy aster
FORB	ASSP	Aster sp.	Aster
FORB	ASSP1	Astragalus sp.	Milk-vetch
FORB	BASA	Balsamorhiza sagittata	Arrowleaf balsamroot
FORB	CAAP	Calochortus apiculatus	Three-spot mariposa lily
FORB	CARO	Campanula rotundifolia	Common harebell
FORB	CAMI	Castilleja miniata	Indian paintbrush
FORB	CASP	Castilleja sp.	Paintbrush
FORB	CASP3	Calochortus sp.	Mariposa lily
FORB	CLOC	Clematis occidentalis/columbiana	Blue clematis
FORB	CLUN	Clintonia uniflora	Queen cup beadlily
FORB	COPA	Collinsia parviflora	Small-flowered blue-eyed Mary
FORB	COCA	Cornus canadensis	Bunchberry dogwood
FORB	COCA2	Conyza canadensis	Horseweed
FORB	COSP	Corallorhiza sp.	Coral-root
FORB	CRSP	Crepis sp.	Hawksbeard species
FORB	DIHO	Disporum hookeri	Hooker fairy-bell
FORB	EPAN	Epilobium angustifolium	Fireweed
FORB	EPSP	Epilobium sp.	Epilobium
FORB	FRVE	Fragaria vesca	Woods strawberry
FORB	FRVI	Fragaria virginiana	Wild strawberry
FORB	GABO	Galium boreale	Northern bedstraw
FORB	GATR	Galium triflorum	Sweetscented bedstraw
FORB	GERI	Geum rivale	Water avens
FORB	GOOB	Goodyera oblongifolia	Rattlesnake plantain
FORB	HELA	Heracleum lanatum	Cow parsnip
FORB	HIAL2	Hieracium albertinum	Western hawkweed
FORB	HIAL	Hieracium albiflorum	White-flowered hawkweed
FORB	HIUM	Hieracium umbellatum	Narrow-leaved hawkweed

FORB	HECY	Heuchera cylindrica	Roundleaf alumroot
FORB	ILRI	Iliamna rivularis	Mountain hollyhock
FORB	LASP	Lathyrus sp.	Peavine
FORB	LOCO	Lotus corniculatus	Bird's-foot trefoil
FORB	LODI	Lomatium dissectum	Fern-leaved lomatium
FORB	LOTR	Lomatium triternatum	Nine-leaved lomatium
FORB	LUSE	Lupinus sericeus	Silky lupine
FORB	LUPN	Lupinus sp.	Lupine
FORB	MEFA	Medicago falcata	Yellow lucerne
FORB	MIGR	Microsteris gracilis	Pink twink
FORB	MISP	Mitella sp.	Mitrewort
FORB	OSCH	Osmorhiza chilensis	Mountain sweet-cicely
FORB	PEDE	Penstemon deustus	Hot-rock penstemon
FORB	PELY	Penstemon lyallii	Lyall's penstemon
FORB	PEWI	Penstemon wilcoxii	Wilcox's penstemon
FORB	PENS	Penstemon sp.	Penstemon species
FORB	PHHA	Phacelia hastata	Silverleaf phacelia
FORB	POPU	Polemonium pulcherrimum	Jacob's-ladder
FORB	PYAS	Pyrola asarifolia	Common pink wintergreen
FORB	PYSE	Pyrola secunda	One-sided wintergreen
FORB	PYSP	Pyrola sp.	Wintergreen
FORB	SELA	Sedum lanceolatum	Lance-leaved stonecrop
FORB	SETR	Senecio triangularis	Arrowleaf groundsel
FORB	SMRA	Smilacina racemosa	False Solomon's seal
FORB	SMST	Smilacina stellata	Starry Solomon's seal
FORB	SOCA	Solidago canadensis	Canada goldenrod
FORB	STSP	Stellaria sp.	Starwort
FORB	TAOF	Taraxacum officinale	Common dandelion
FORB	THOC	Thalictrum occidentale	Western meadowrue
FORB	TITR	Tiarella trifoliata	Coolwort foamflower
FORB	TIUN	Tiarella unifoliata	One-leaved foamflower
FORB	TRDU	Tragopogon dubius	Yellow salsify
FORB	TROV	Trillium ovatum	Trillium
FORB	TRRE	Trifolium repens	White clover
FORB	VESP	Veronica sp.	Veronica
FORB	VIAM	Vicia americana	American vetch
FORB	VIAD	Viola adunca	Hook violet
FORB	VIGL	Viola glabella	Stream violet
FORB	VIOR	Viola orbiculata	Round-leaved violet
FORB	XETE	Xerophyllum tenax	Beargrass
NOXS	CEST	Centaurea stoebe	spotted knapweed

NOXS	CIAR4	Cirsium arvense	Canada thistle
NOXS	CIVU	Cirsium vulgare	Bull thistle
NOXS	THIS	Cirsium sp.	Thistle
NOXS	LASE	Lactuca serriola	Prickly lettuce
FERN	POMU	Polystichum munitum	Western swordfern
FERN	PTAQ	Pteridium aquilinum	Bracken fern
FERN	EQAR	Equisetum arvense	Field horsetail
GRAS	BRTE	Bromus tectorum	Cheatgrass
GRAS	BRSP	Bromus sp.	Brome
GRAS	CACA	Calamagrostis canadensis	Bluejoint reedgrass
GRAS	CARU	Calamagrostis rubescens	Pinegrass
GRAS	CAGE	Carex geyeri	Elk sedge
GRAS	CARX	Carex sp.	Sedge
GRAS	ELGL	Elymus glaucus	Blue wildrye
GRAS	FEID	Festuca idahoensis	Idaho fescue
GRAS	KOMA	Koeleria macrantha	Junegrass
GRAS	LUPA	Luzula parviflora	Millet woodrush
GRAS	PHPR	Phleum pratense	Timothy
GRAS	POSA	Poa sandbergii	Sandberg bluegrass
GRAS	POSP	Poa sp.	Bluegrass
GRAS	PSSP	Pseudoregneria spicata	Bluebunch wheatgrass
GRAS	TRSP	Trisetum spicatum	Spike trisetum
GRAS	GRASS		Grass
GRAS	GRASS 1		Grass 1
CLAS	MOSS		Moss
CLAS	LICEN		Lichen
CLAS	FUNGI		Fungi
CLAS	FUNGI1		Fungi 1
CLAS	FUNGI2		Fungi 2
UNKN	UNKNJ		Unknown plant (Cooney 9; 2014)

Appendix 2

Data used in the analysis.

	MTBS	green_cover	NPV_cover	NPV_char_cover	rock_cover	soil_cover
B1	3	0.57	0.25	0.01	0.1	0.08
B2	2	0.6	0.4	0	0	0
B3	1	0.42	0.55	0.1	0.03	0
B4	1	0.84	0.1	0	0.01	0.05
B5	3	0.84	0.1	0.1	0.03	0.03
B6	1	0.79	0.2	0	0	0.01
C1	3	0.72	0.15	0.01	0.03	0.1
C10	3	0.75	0.25	0	0	0
C2	1	0.25	0.63	0	0	0.02
C3	1	0.5	0.35	0.7	0	0.15
C4	1	0.22	0.76	0.01	0	0.02
C5	2	0.65	0.35	0.2	0	0
C6	1	0.85	0.15	0.01	0	0
C7	1	0.5	0.1	0	0.25	0.15
C8	1	0.5	0.5	0.05	0	0
C9	1	0.13	0.02	0.4	0.2	0.65
R1	3	0.75	0.25	0.05	0	0
R10	3	0.81	0.07	0.8	0.1	0.02
R11	2	0.3	0.7	0.25	0	0
R2	1	0.45	0.55	0.01	0.02	0
R3	1	0.2	0.76	0.05	0.02	0.02
R4	2	0.89	0.08	0.05	0	0.03
R5	1	0.88	0.1	0	0.01	0.01
R6	2	0.75	0.25	0.05	0	0
R7	1	0.75	0.25	0	0	0
R8	3	0.13	0.3	0.05	0.55	0.02
R9	3	0.19	0.75	0	0.02	0.04
W2	3	0.8	0.1	0.01	0.05	0.05
W3	1	0.74	0.2	0.25	0.01	0.05
W4	3	0.65	0.35	0.05	0	0
W5	1	0.9	0.1	0	0	0
W6	3	0.84	0.15	0.02	0.01	0
W7	2	0.9	0.1	0.9	0	0
W8	1	0.69	0.2	0.05	0.01	0.1

	species_richness	1_hour_fuels	10_hour_fuels	100_hour_fuels	litter_depth	duff_depth
B1	9	0	0	0	11	9
B2	18	0.04	0.07	0.5	16	14
B3	24	0.02	0.02	3	11	2
B4	28	0.01	0	0	21	0
B5	16	0.03	0.2	0	15	2
B6	23	0.07	0.03	0.2	12	16
C1	27	0.3	0.5	0.5	9	2
C10	49	0.7	0.8	2	40	17
C2	35	0.1	0.05	0.3	31	6
C3	29	0.2	2	1	9	9
C4	22	0.01	0.05	0	16	0
C5	20	0.3	0.6	3	20	13
C6	16	0.1	0.5	2	18	8
C7	22	0.01	0.03	0	3	0
C8	35	0.1	0.04	0.02	22	8
C9	43	0.01	0.01	0.01	0	0
R1	20	0.07	0.03	0.1	3	15
R10	39	0.07	0.1	0.01	5	19
R11	31	1	0.05	0.5	20	20
R2	16	0.1	0.07	0.05	0	0
R3	21	0.1	1	1	17	9
R4	19	0.06	0.08	0.1	4	4
R5	23	0.06	0	0	5	2
R6	32	0.6	0.3	0.5	64	26
R7	31	0.04	0.07	0.4	17	11
R8	49	0.5	0.7	3	9	24
R9	43	0.5	0.8	0.4	4	9
W2	31	0.07	0.03	0.07	7	2
W3	18	0.07	0.03	0.07	7	2
W4	26	0.03	0.07	0.3	13.1	3
W5	29	0.1	0.01	0.3	3	10
W6	22	0.7	0.9	0.06	27	11
W7	34	0.04	0.04	0.08	19	13
W8	30	0.3	0.2	0.06	8	9

	duff_depth	healthy_tree_density	unhealthy_tree_density	dead_tree_density
B1	9	0	0	1200
B2	14	250	0	300
B3	2	50	0	100
B4	0	50	0	0
B5	2	0	0	100
B6	16	0	0	700
C1	2	0	0	50
C10	17	0	0	450
C2	6	750	0	50
C3	9	0	0	200
C4	0	250	0	0
C5	13	0	0	700
C6	8	400	150	350
C7	0	0	0	0
C8	8	300	50	0
C9	0	0	0	0
R1	15	0	0	200
R10	19	0	0	50
R11	20	100	0	1100
R2	0	800	50	50
R3	9	50	0	0
R4	4	0	0	300
R5	2	50	0	0
R6	26	0	0	100
R7	11	250	0	0
R8	24	0	0	50
R9	9	0	0	150
W2	2	0	0	700
W3	2	600	0	0
W4	3	0	0	250
W5	10	550	0	50
W6	11	0	0	600
W7	13	0	0	250
W8	9	350	200	200

	1000_hour_fuels	shrub_cover	live_sapling_density	live_seedling_density
B1	13	0	0	5833.333
B2	50	500	2000	12666.67
B3	100	100	0	1000
B4	0	0	0	0
B5	6	1500	1200	2100
B6	35	200	300	10833.33
C1	40	0	400	3333.333
C10	35	400	600	45333.33
C2	3	100	0	8.333333
C3	23	100	2000	10000
C4	3	0	0	500
C5	27	700	1400	1666.667
C6	20	0	0	4666.667
C7	0	0	400	550
C8	1	800	500	2733.333
C9	0	0	100	683.3333
R1	12	1000	1800	355.5556
R10	23	1500	400	566.6667
R11	60	7000	0	92000
R2	1	500	100	83.33333
R3	28	2000	1100	4666.667
R4	50	3000	1300	2500
R5	9	1000	100	1133.333
R6	90	2000	0	1033.333
R7	12.5	1200	900	2750
R8	50	100	0	266.6667
R9	60	500	500	5533.333
W2	30	100	0	1291.667
W3	4	200	6900	18666.67
W4	100	200	26800	20000
W5	10	300	200	1000
W6	15	300	4300	30666.67
W7	40	800	100	43333.33
W8	1	0	0	6833.333

Appendix 3. Density graphs for the data used in the MANOVA, group 1 and 2 and seedling density.

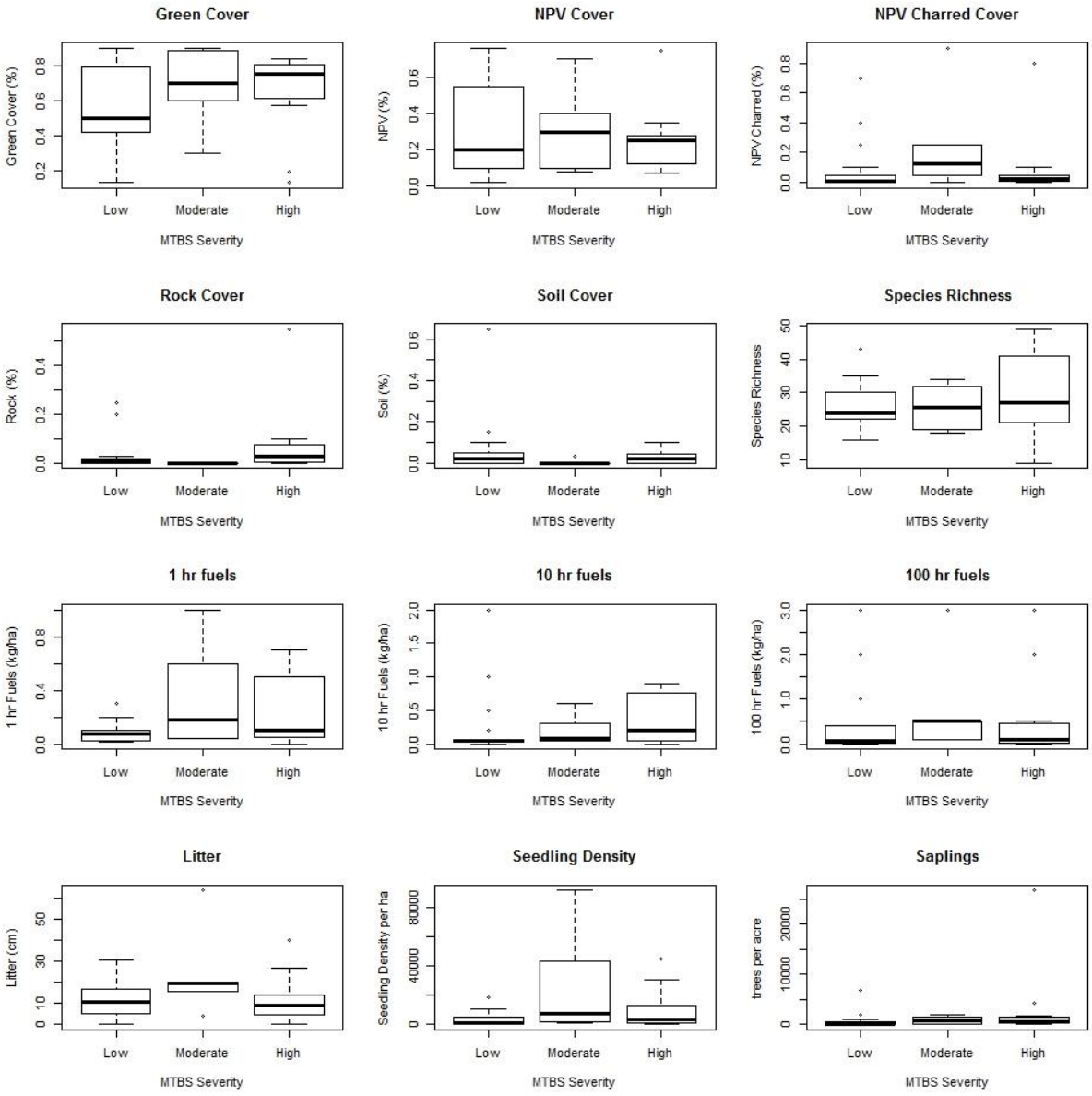

Appendix 4. Correlations for the species to the axis produced by the ordination. Pearson correlation coefficient, r-squared and Kendall's tau are reported.

Axis	1			2			3		
	r	r-sq	tau	r	r-sq	tau	r	r-sq	tau
ABLA	-0.011	0	-0.174	0.023	0.001	0.174	-0.327	0.107	-0.188
ACGL	0.135	0.018	0.293	0.003	0	0.094	-0.312	0.098	-0.176
ACMI	0.011	0	-0.041	0.11	0.012	0.127	0.204	0.042	0.178
ALSI	-0.252	0.064	-0.131	0.07	0.005	0.077	-0.257	0.066	-0.167
AMAL	0.403	0.163	0.33	-0.311	0.096	-0.176	-0.249	0.062	-0.145
ANMA	-0.478	0.228	-0.439	0.206	0.042	0.091	0.032	0.001	-0.127
ANMI	-0.187	0.035	-0.15	-0.438	0.192	-0.378	-0.144	0.021	-0.173
ANRA	-0.006	0	0.115	0.425	0.181	0.259	0.074	0.006	0.19
APAN	0.386	0.149	0.344	-0.092	0.008	-0.21	-0.353	0.125	-0.281
ARCO	-0.11	0.012	-0.098	0.448	0.201	0.493	-0.196	0.038	-0.14
ARUV	0.41	0.168	0.323	-0.052	0.003	0.039	-0.173	0.03	-0.047
ASCO	0.147	0.022	0.187	-0.039	0.002	0.064	0.289	0.083	0.128
ASSP	-0.014	0	0.025	-0.275	0.076	-0.036	-0.149	0.022	-0.036
BERE	0.629	0.396	0.558	-0.301	0.09	-0.107	0.175	0.031	0.03
BRSP	-0.306	0.094	-0.313	0.255	0.065	0.233	-0.102	0.01	-0.075
BRTE	0.357	0.127	0.372	0.028	0.001	-0.163	0.118	0.014	0.027
CAGE	-0.15	0.022	-0.195	-0.329	0.108	-0.136	0.382	0.146	0.186
CAMI	0.234	0.055	0.218	-0.051	0.003	-0.154	0.031	0.001	0.146
CARU	0.196	0.038	0.257	0.445	0.198	0.307	0.431	0.186	0.328
CARX	0.333	0.111	0.388	0.127	0.016	0.152	0.328	0.108	0.069
CASP	-0.071	0.005	0.052	-0.239	0.057	0.023	0.007	0	0.127
CEST	0.035	0.001	0.292	-0.204	0.042	-0.113	-0.028	0.001	-0.02
CEVE	0.017	0	0.041	-0.009	0	-0.041	0.086	0.007	0.23
CHUM	-0.164	0.027	-0.146	-0.09	0.008	-0.162	-0.139	0.019	-0.123
CLUN	-0.286	0.082	-0.217	0.043	0.002	0.03	-0.347	0.121	-0.201
COPA	0.246	0.061	0.183	-0.009	0	-0.028	0.191	0.037	0.174
DIHO	-0.065	0.004	0.043	-0.058	0.003	0	-0.097	0.009	-0.085
ELGL	-0.337	0.113	-0.337	-0.035	0.001	-0.023	-0.074	0.005	0.003
EPAN	-0.481	0.231	-0.449	-0.132	0.017	-0.075	-0.195	0.038	-0.06
EPSP	0.396	0.156	0.232	-0.224	0.05	-0.007	0.06	0.004	-0.007
FEID	0.195	0.038	-0.075	0.082	0.007	0.02	0.168	0.028	0.162
FRVE	0.009	0	0.012	0.163	0.027	0.108	-0.044	0.002	-0.044
FRVI	-0.036	0.001	0.14	-0.059	0.003	-0.033	-0.009	0	-0.018
FUNGI	-0.324	0.105	-0.299	0.041	0.002	0.028	-0.044	0.002	-0.052
GABO	0.027	0.001	0.091	-0.184	0.034	0.064	0.001	0	-0.091
GATR	-0.251	0.063	-0.248	0.147	0.022	0.036	-0.185	0.034	-0.129
GRASS	0.121	0.015	-0.036	-0.16	0.026	-0.241	-0.069	0.005	-0.051

HIAL	-0.536	0.287	-0.478	0.205	0.042	0.127	-0.117	0.014	-0.064
HIAL2	-0.07	0.005	-0.07	-0.123	0.015	-0.124	-0.224	0.05	-0.086
ILRI	-0.19	0.036	-0.134	-0.068	0.005	0	0.055	0.003	0.016
LAOC	0.067	0.004	-0.048	0.179	0.032	0.028	-0.249	0.062	-0.308
LIBO2	-0.057	0.003	0.083	0.011	0	0.055	-0.034	0.001	-0.044
LICEN	0.238	0.057	0.187	-0.195	0.038	-0.151	-0.148	0.022	-0.093
LOUT2	-0.063	0.004	-0.069	0.021	0	-0.167	0.106	0.011	-0.023
LUPN	0.124	0.015	0.282	0.227	0.051	0.16	0.16	0.026	0.282
MEFA	-0.178	0.032	-0.14	-0.313	0.098	-0.357	-0.11	0.012	-0.068
MEFE	-0.366	0.134	-0.35	-0.227	0.051	-0.186	0.089	0.008	0.173
MISP	-0.018	0	-0.086	0.359	0.129	0.338	0.04	0.002	0.086
MOSS	-0.56	0.314	-0.524	-0.635	0.404	-0.425	-0.03	0.001	-0.002
OSCH	0.089	0.008	0.072	0.187	0.035	0.114	-0.031	0.001	-0.057
PAMY	-0.114	0.013	0.042	0.24	0.057	0.033	-0.059	0.004	-0.042
PENS	0.035	0.001	-0.021	-0.064	0.004	-0.072	0.463	0.214	0.272
PHMA	0.672	0.451	0.484	-0.176	0.031	-0.031	-0.096	0.009	-0.061
PICO	0.052	0.003	0	0.186	0.035	-0.044	0.294	0.086	0.312
PIEN	-0.315	0.099	-0.314	0.062	0.004	0.016	-0.282	0.079	-0.258
POSA	0.185	0.034	0.199	0.32	0.102	0.254	-0.259	0.067	-0.21
POSP	-0.049	0.002	0.027	-0.147	0.022	-0.009	-0.126	0.016	-0.109
POTR	-0.319	0.102	-0.214	-0.265	0.07	-0.079	0.114	0.013	0.205
PSME	0.073	0.005	0.168	0.204	0.042	0.245	-0.097	0.009	-0.068
PSSP	0.267	0.071	0.009	-0.251	0.063	-0.118	-0.158	0.025	-0.1
PTAQ	-0.223	0.05	-0.175	-0.024	0.001	-0.046	-0.197	0.039	-0.26
PYAS	-0.106	0.011	-0.059	-0.034	0.001	-0.067	-0.295	0.087	-0.202
PYSE	-0.265	0.07	-0.203	-0.1	0.01	-0.127	0.01	0	0.023
RILA	-0.304	0.092	-0.236	0.234	0.055	0.236	-0.249	0.062	-0.11
RIVI	0.22	0.048	0.185	0.017	0	0.014	0.299	0.09	0.212
ROSA	0.315	0.099	0.332	0.122	0.015	0.077	-0.206	0.042	-0.29
RUPA	-0.175	0.031	-0.095	0.167	0.028	0.232	0.01	0	-0.137
SALX	-0.439	0.193	-0.404	-0.123	0.015	-0.089	-0.445	0.198	-0.268
SMRA	0.142	0.02	0.186	-0.109	0.012	-0.02	0.368	0.136	0.218
SMST	-0.144	0.021	-0.041	0.027	0.001	0.006	-0.426	0.181	-0.353
SOCA	-0.248	0.061	-0.117	-0.179	0.032	-0.037	-0.255	0.065	-0.148
SOSC2	-0.161	0.026	-0.221	0.254	0.065	0.257	-0.069	0.005	-0.176
SPBE	0.476	0.226	0.556	0.223	0.05	0.159	-0.354	0.126	-0.12
SYAL	0.274	0.075	0.321	-0.368	0.136	-0.111	-0.204	0.042	-0.133
TAOF	-0.199	0.039	-0.147	-0.088	0.008	0.012	-0.08	0.006	-0.051
THOC	0.074	0.006	-0.069	0.335	0.112	0.245	-0.129	0.017	-0.078
VAGL	-0.385	0.148	-0.291	0.274	0.075	0.271	0.303	0.092	0.171
VASC	-0.178	0.032	-0.142	-0.384	0.148	-0.163	0.185	0.034	0.149

VIAM	-0.013	0	-0.068	0.222	0.049	0.041	0.066	0.004	0.077
VIGL	-0.142	0.02	-0.067	0.335	0.112	0.305	-0.318	0.101	-0.226
VIOR	-0.393	0.154	-0.292	0.001	0	0.061	-0.372	0.139	-0.243
XETE	-0.218	0.047	-0.24	-0.081	0.006	-0.048	0.626	0.392	0.348